A Quantitative Analysis of Image Segmentation Techniques/Algorithms Using OCT Retinal Images in the Search of Highest Accuracy to Support the Field of Ophthalmology

Course: Computer science – G400

By: Cameron Dheer

Date: 11/08/2022

Contents

Contents

Table of Tables

Table of Figures

Executive Summary

This dissertation study offers a quantitative analysis of image segmentation techniques/algorithms using OCT retinal images in the search of highest accuracy to support the field of ophthalmology.

Challenges with OCT image scans have been explored in detail to understand the complexities with regards to inherent noise and image quality that cause issues in the interpretation of OCT scan images for diagnosis and monitoring of a wide range of health conditions. An overview of techniques to combat these challenges through image segmentation have been studied. In total, four image segmentation algorithms/techniques have been carefully selected (Canny Edge Detection, K-Means Clustering, Simple Thresholding, and Otsu's Thresholding) for a comparison to ground truths that were clinically annotated. The newly created segments are evaluated using the Dice Coefficient metric to measure pixel-wise accuracy of the algorithm.

In evaluating all four algorithms, Canny Edge Detection has proven to have the most pixel-wise agreement in creating segments that intersect more greatly with the ground truth images. Although this algorithm did not produce any exact matches, it did deliver a dice coefficient of 0.592. This high level of overlap validates the algorithm can identify areas of interest such as retinal layers, features, and abnormalities that are relevant to ophthalmologists. However, there are areas of interest that exist on the original unprocessed image which are not identified automatically by the algorithm. As a result, this could limit diagnostic capability and a brief review of the original OCT image may still be required by an ophthalmologist. An ophthalmologist would need to advise on how successful the algorithm really is in a clinical setting.

An image segmentation technique/algorithm that produced a perfect dice coefficient of 1 was always going to be difficult to find but an algorithm was identified that performs well. The goal of this dissertation study was to find an image segmentation technique/algorithm that was the most accurate and this was discovered from the 4 that were analysed.

To conclude, whilst it has been found Canny Edge Detection algorithm works well with OCT retinal scan data, the results obtained do depend on the quality of the OCT image scans in the first place. The better the quality, the better the resulting segmented images from the techniques/algorithms

Changes for the Resit

This report and technical work has been submitted for the first time this summer.

1. Background

1.1 Introduction

The focus of this study is centred on Optical Coherence Tomography (OCT) scans that are performed on the human eye. Eyes are one of the main five human senses and the eye has over 130 million sensors in the retina[1]. Figure 1 provides a cross section of the human eye. By assessing the eye, they offer a window into our health via changes that take place.

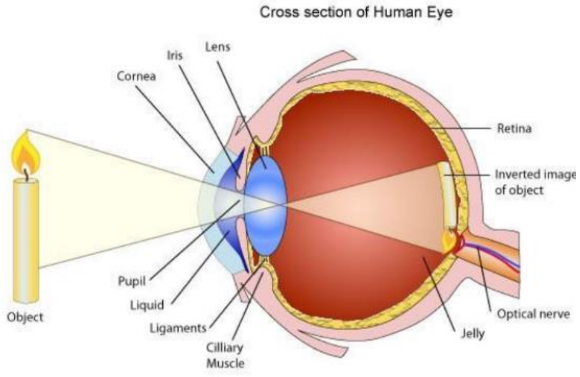

Figure 1: Cross section of human eye. Source: http://rmsphotographygcse.weebly.com

Eyes offer insight into possible infection, diabetes, high cholesterol, high blood pressure and much more. The ability for ophthalmologists to interpret OCT scans is critical to supporting a diagnosis and better health outcomes.

The goal of this dissertation study is to evaluate several image segmentation techniques/algorithms in the search of the most accurate segmentation technique/algorithm for OCT image scans.

1.2 What is an OCT scan?

An OCT scan is a type of imaging test that is non-invasive and has wide medical use. Bin et al.[2] cite it as being "considered an indispensable diagnostic tool in ophthalmology, dermatology, and cardiology". For the purposes of this dissertation study, the focus will be on using OCT for early diagnosis or monitoring of ocular conditions. Examples of OCT scan images have been provided in figures 2 and 3.

[1]Roger Cicala, "The Camera Versus the Human Eye", PetaPixel, NOV 17, 2012, https://petapixel.com/2012/11/17/the-camera-versus-the-human-eye/#:~:text=The%20eye%20has%20130%20million,brain%20at%20any%20given%20instant

[2] Bin Qiu, Zhiyu Huang, Xi Liu, Xiangxi Meng, Yunfei You, Gangjun Liu, Kun Yang, Andreas Maier, Qiushi Ren, and Yanye Lu, "Noise reduction in optical coherence tomography images using a deep neural network with perceptually-sensitive loss function", Biomed Opt Express, 2020 Feb 1

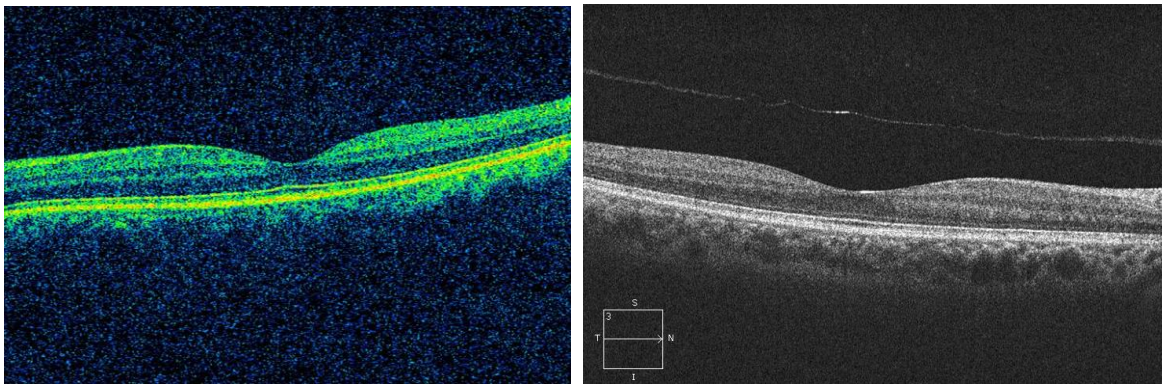

Figure 2: OCT scans from Optical Coherence Tomography Image Retinal Database shared by a study from Gholami, et al. [3]

Figure 3: OCT scans from Optical Coherence Tomography Image Retinal Database shared by a study from Gholami, et al.

OCT takes cross-section images of your retina using light waves. According to the American Academy of Ophthalmology[4], this type of image is used by Ophthalmologists to see each of the retina's distinct layers, and allows ophthalmologists to map and measure their thickness that help with diagnosis. Some of the conditions that can be diagnosed include glaucoma, age-related macular degeneration (AMD), diabetic eye disease, and other diseases of the retina.

The procedure for an OCT from start to end lasts approximately 10 minutes[5]. It is a painless procedure where a patient places their chin into a chin rest and keeps their eye open, looks at a target - often a blinking dot or a small picture. The OCT machine then scans your eye while the patient is fixated on the light inside of the machine. It is at the ophthalmologist's discretion as to whether the eyes are dilated during the procedure or not.

According to Dr. Russel Lazarus from Optometrists Network, OCT scans are typically performed on those over the age of 25, or at risk of developing ocular disease, an ophthalmologist may recommend an OCT exam as part of an annual eye exam[6]. Having regular OCT scans will enable ophthalmologists to compare the images from previous years to detect any abnormalities or thickening of retinal layers.

1.3 History & Current State of Retinal Image Processing

[3] Peyman Gholami, Priyanka Roy, Mohana Kuppuswamy Parthasarathy, Vasudevan Lakshminarayanan, "OCTID: Optical Coherence Tomography Image Database", arXiv preprint arXiv:1812.07056, (2018).
[4] David Turbert, "What Is Optical Coherence Tomography?", American Academy of Ophthalmology, Mar. 08, 2022, https://www.aao.org/eye-health/treatments/what-is-optical-coherence-tomography
[5] Dr. Louis P. Bahoshy, "What is Optical Coherence Tomography", Stoney Creek Eye Care, https://stoneycreekeyecare.com/what-is-optical-coherence-tomography-oct/#:~:text=From%20start%20to%20finish%2C%20an,OCT%20machine%20scans%20your%20eye
[6] Dr. Russel Lazarus, "What is an OCT Eye Exam", Optometrists Network, August 23, 2020, https://www.optometrists.org/general-practice-optometry/guide-to-eye-exams/eye-exams/what-is-an-oct-eye-exam/

The first to publish a method for retinal image analysis was Matsui et al., this was primarily focused on vessel segmentation[7]. Next, the first method to detect and segment abnormal structures was reported in 1984, when Baudoin et al. described an image analysis method for detecting microaneurysms, a characteristic lesion of diabetic retinopathy[8]. Abramoff et al.[9], cite "in the 1990s that the field dramatically changed with the development of digital retinal imaging and the expansion of digital filter-based image analysis techniques". Retinal imaging is now therefore a critical centrepiece of clinical care and management of patients with retinal diseases.

1.4 Eye Anatomy

To further explore OCT image segmentation further, it is important to have foundational knowledge in the eye anatomy to support what is identified in the segmented images and ground truth images.

Abramoff et al.[10] provide an insightful overview and the below is an excerpt from the study including figures:

> " A brief review of gross eye anatomy is in place (figure 4). The visible parts of the eye include the transparent cornea, the normally white sclera, the coloured (blue, green, brown or a mixture of these) iris, and an opening in the iris, the normally black pupil. A ray of light, after passing through the cornea, which partially focuses the image, passes through the anterior chamber, the pupil, the lens, which focuses the image further, the vitreous and is then focused on the retina. The retina itself is supported by its retinal pigment epithelium, which is normally opaque, the choroid and the sclera. The blood supply of the retina is primarily (~65%) through the choroid and secondarily (~35%) through the retinal vasculature which lies on top of the retina. It is useful to divide the retina and choroid into the following layers:

[7] M. Matsui, T. Tashiro, K. Matsumoto, and S. Yamamoto, "A study on automatic and quantitative diagnosis of fundus photographs. I. Detection of contour line of retinal blood vessel images on color fundus photographs (author's transl.)," Nippon Ganka Gakkai Zasshi, vol. 77, no. 8, pp. 907–918, 1973, [Online]. Available: PM:4594062.

[8] G. Quellec, M. Lamard, P. M. Josselin, G. Cazuguel, B. Cochener,and C. Roux, "Optimal wavelet transform for the detection of microaneurysms in retina photographs," IEEE Trans. Med. Imaging, vol. 27, no. 9, pp. 1230–1241, Sep. 2008.

[9] Michael D. Abràmoff, Senior Member, IEEE, Mona K. Garvin, Member, IEEE, and Milan Sonka, Fellow, IEEE, "Retinal Imaging and Image Analysis", IEEE REVIEWS IN BIOMEDICAL ENGINEERING, VOL. 3, 2010

[10] Michael D. Abràmoff, Senior Member, IEEE, Mona K. Garvin, Member, IEEE, and Milan Sonka, Fellow, IEEE, "Retinal Imaging and Image Analysis", IEEE REVIEWS IN BIOMEDICAL ENGINEERING, VOL. 3, 2010

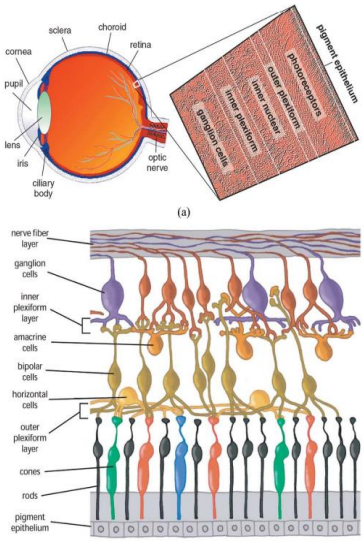

Figure 4: Illustration of eye anatomy and retinal layers - (a) Cross-sectional view of eye and its major structures (b) Schematic drawing of cellular layers of retina.

It is useful to divide the retina and choroid into the following layers:

1. Internal limiting membrane;
2. Nerve fiber layer (the axons of the ganglion cells, that transmit the visual signal to the lateral geniculate nucleus and thence the visual cortex);
3. Ganglion cell layer (the cell bodies of the ganglion cells);
4. Inner plexiform layer (the axons of the bipolar cells);
5. inner nuclear layer (the cell bodies of the bipolar and horizontal cells);
6. Outer plexiform layer (the dendrites of the horizontal cells and the inner segments of the rod and cone photoreceptor cells);
7. Outer nuclear layer (cell bodies—outer segments—of the photoreceptor cells);
8. External limiting membrane;
9. Pigment epithelium;
10. Bruch's membrane;
11. Capillary choroid (capillaries of the choroid);
12. Choroid plexus."

Each retinal layer does offer insights into health and thus, it is critical to evaluate each layer and any associated abnormalities. Retinal layers are visible on OCT image scans and will be discussed at length throughout the upcoming sections. Figure 5 shows an OCT image scan from The University of Iowa Institute for Vision Research Ophthalmic Image Analysis study[11], which has been annotated to show the 12 layers in the retina.

[11] Abrámoff, Kwon, Sonka team, "Ophthalmic Image Analysis", The Iowa Institute for Biomedical Imaging, https://www.iibi.uiowa.edu/ophthalmic-analysis

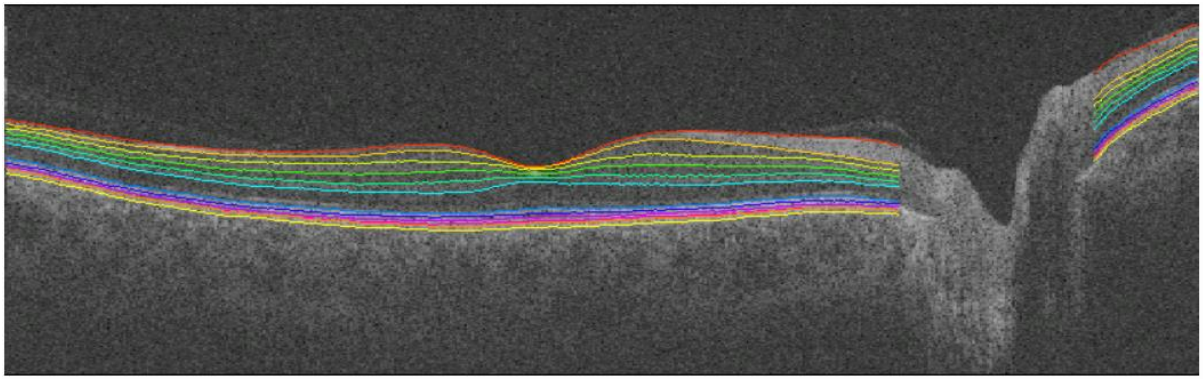

Figure 5: OCT image scans segmentation results from The University of Iowa Institute for Vision Research Ophthalmic Image Analysis

To further support this, figure 6 from Luo et al., offers a second view with smaller annotation into the retinal layers displayed in OCT image scans[12]. Without image segmentation technique/algorithm distinguishing the layers, it is hard to identify the layers through direct observation due to the complexity of the scanned image.

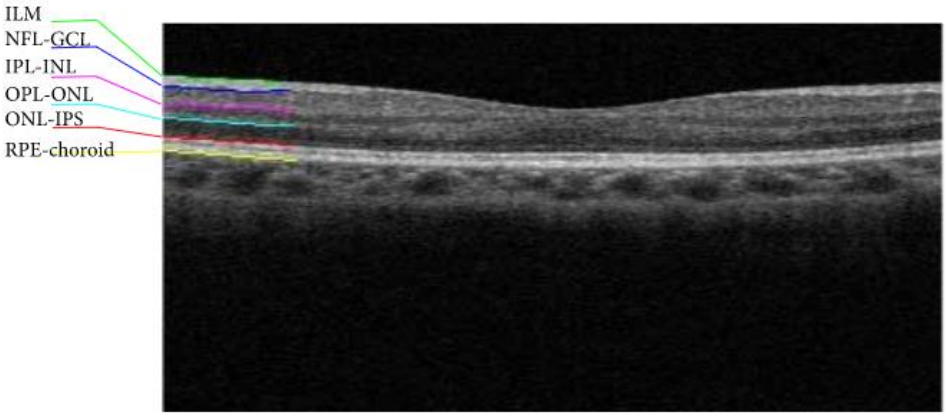

Figure 6: The retinal layers in a representative cross-sectional SD-OCT image scan .

Abràmoff et al., note “many important diseases manifest themselves in the retina and originate either in the eye, the brain, or the cardiovascular system”[13]. With the eye offering so much insight into one's health, this highlights even more the importance of accuracy needed in image segmentation to support ophthalmologists in detecting abnormalities and changes.

1.5 Challenges with OCT Image Scans

[12] Su Luo, Jing Yang, Qian Gao, Sheng Zhou, Chang’an A. Zhan, "The Edge Detectors Suitable for Retinal OCT Image Segmentation", Journal of Healthcare Engineering, vol. 2017, Article ID 3978410, 13 pages, 2017. https://doi.org/10.1155/2017/3978410

[13] Michael D. Abràmoff, Senior Member, IEEE, Mona K. Garvin, Member, IEEE, and Milan Sonka, Fellow, IEEE, "Retinal Imaging and Image Analysis", IEEE REVIEWS IN BIOMEDICAL ENGINEERING, VOL. 3, 2010

OCT image scans suffer from a granular pattern and are inherently noisy[14]. According to Bin et al.[15] OCT image scans are highly "susceptible to speckle noise that deteriorates contrast and the detail of structural information in OCT image scans, thus imposing significant limitations on the diagnostic capability". Poor image quality can also impact the accuracy of segmentation of retinal layers and the measurements of tissue thickness. Therefore, restricting the process of interpretation and ultimately affecting clinical decisions[16]. Figure 7 shows speckle noise that is frequently present in OCT image scans.

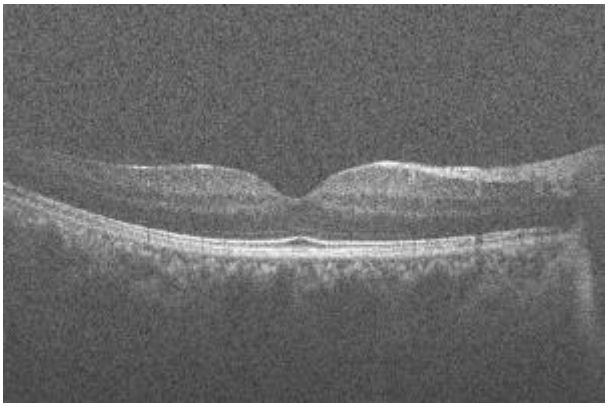

Figure 7: Typical retinal OCT image scans degraded by speckle noise.

With speckle noise in OCT image scans, it can cause tremendous difficulty in precise identification of retinal layers through the use of image segmentation techniques/algorithms as well as when observing directly.

2. Image Analysis & Image Segmentation

Image analysis is the extraction of meaningful information from images; mainly from digital images by means of digital processing techniques[17]. These techniques have expansive application across science and industry. Among the many techniques, image segmentation is one of these. Other aspects include objection recognition, motion detection, video tracking to name a few.

[14] Raheleh Kafieh, Hossein Rabbani, and Saeed Kermani1, "A Review of Algorithms for Segmentation of Optical Coherence Tomography from Retina", J Med Signals Sens v.3(1); Jan-Mar 2013 PMC3785070

[15] Bin Qiu, Zhiyu Huang, Xi Liu, Xiangxi Meng, Yunfei You, Gangjun Liu, Kun Yang, Andreas Maier, Qiushi Ren, and Yanye Lu, "Noise reduction in optical coherence tomography images using a deep neural network with perceptually-sensitive loss function", Biomed Opt Express. 2020 Feb 1; 11(2): 817–830.

[16] Sripad Krishna Devalla, Giridhar Subramanian, Tan Hung Pham, Xiaofei Wang, Shamira Perera, Tin A. Tun, Tin Aung, Leopold Schmetterer, Alexandre H. Thiéry & Michaël J. A. Girard, "A Deep Learning Approach to Denoise Optical Coherence Tomography Images of the Optic Nerve Head", Scientific Reports, Published: 08 October 2019

[17] Solomon, C.J., Breckon, T.P. (2010). "Fundamentals of Digital Image Processing: A Practical Approach with Examples in Matlab". Wiley-Blackwell. doi:10.1002/9780470689776

Image segmentation according to Wikipedia[18] is the actual process of "partitioning a digital image into multiple segments, also known as image objects[19]. The goal of segmentation is to simplify and/or change the representation of an image into something that is more meaningful and easier to analyse[20]"- reducing the complexity of the image. Image segmentation therefore locates objects and boundaries (lines, curves, etc.) in images. The process includes "assigning a label to every pixel in an image such that pixels with the same label share certain characteristics. The result of image segmentation is a set of segments that collectively cover the entire image, or a set of contours extracted from the image".

This field has become a rapidly growing area using domain-specific knowledge to effectively solve image segmentation problems in specific application areas. There are multiple groups of image segmentation, they include:

- Semantic segmentation is an approach detecting, for every pixel, belonging class of the object[21]. For example, when each animal in a figure is segmented as one object and background as one object.
- Instance segmentation is an approach that identifies, for every pixel, a belonging instance of the object. It detects each distinct object of interest in the image[22]. For example, when each animal in a figure is segmented as an individual object.
- Panoptic segmentation combines semantic and instance segmentation. Like semantic segmentation, panoptic segmentation is an approach that identifies, for every pixel, the belonging class. Unlike semantic segmentation, panoptic segmentation distinguishes different instances of the same class[23].

Within these groups, there are several techniques/algorithms for image segmentation. In addition to this, image pre-processing and post-processing techniques exist to further improve results of the image segmentation. It is a complex area of study.

[18] Wikipedia source: https://en.wikipedia.org/wiki/Image_segmentation#:~:text=More%20precisely%2C%20image%20segmentation%20is,same%20label%20share%20certain%20characteristics.

[19] Linda G. Shapiro and George C. Stockman (2001): "Computer Vision", pp 279–325, New Jersey, Prentice-Hall, ISBN 0-13-030796-3

[20] Barghout, Lauren, and Lawrence W. Lee. "Perceptual information processing system." Paravue Inc. U.S. Patent Application 10/618,543, filed July 11, 2003.

[21] Guo, Dazhou; Pei, Yanting; Zheng, Kang; Yu, Hongkai; Lu, Yuhang; Wang, Song (2020). "Degraded Image Semantic Segmentation With Dense-Gram Networks". IEEE Transactions on Image Processing. 29: 782–795. Bibcode:2020ITIP...29..782G. doi:10.1109/TIP.2019.2936111. ISSN 1057-7149. PMID 31449020. S2CID 201753511.

[22] Yi, Jingru; Wu, Pengxiang; Jiang, Menglin; Huang, Qiaoying; Hoeppner, Daniel J.; Metaxas, Dimitris N. (July 2019). "Attentive neural cell instance segmentation". Medical Image Analysis. 55: 228–240. doi:10.1016/j.media.2019.05.004. PMID 31103790. S2CID 159038604

[23] Alexander Kirillov, Kaiming He, Ross Girshick, Carsten Rother, Piotr Dollár (2018). "Panoptic Segmentation". arXiv:1801.00868

2.1 Challenges with Image Segmentation

Kafieh et al.[24] highlight image segmentation is one of the most difficult steps in OCT image scans analysis. There is no single image segmentation method that works equally well across all images. Manual OCT image segmentation therefore is considered the gold standard according to Kafieh et. al., this is where a clinical expert annotates regions of interest. However, this is a time-consuming, and laborious task. It draws great variability as it is dependent on human expertise. Accurate and automated algorithms are desired, but there are no clinical practice standards.

According to a study by Baghaie et. al.[25], there are four major challenges that are encountered in the segmentation of OCT image scans, the below are cited from this study:

1. The presence of speckle noise (as mentioned above section) complicates the process of the precise identification of the retinal layers, therefore most of the image segmentation methods require pre-processing steps to reduce the noise;
2. Intensity of homogeneous areas decreases with increased depth of imaging. This is since the intensity pattern in OCT image scans is the result of the absorption and scattering of light in the tissue;
3. Optical shadows imposed by blood vessels can also affect the performance of segmentation methods;
4. Quality of OCT image scans degrades because of motion artifacts or sub-optimal imaging conditions.

With so many challenges, it has led to greater complexity in successfully locating meaningful image segments in OCT. Pre-processing and post-processing are frequently used methods to assist in overcoming some of these challenges that will be discussed in the section 3.8 for this dissertation's methodology.

3. Image Segmentation Techniques

In the growing field of image segmentation, the number of techniques and algorithms have grown vastly. A high level overview of the classifications is presented in figure 8.

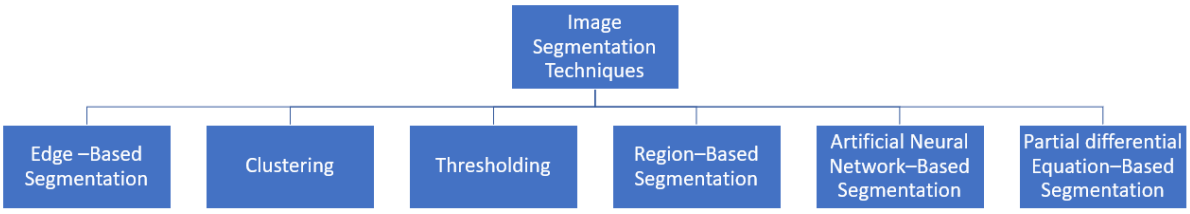

Figure 8: High level classification of image segmentation approaches

[24] Raheleh Kafieh, Hossein Rabbani, and Saeed Kermani, "A Review of Algorithms for Segmentation of Optical Coherence Tomography from Retina", J Med Signals Sens. 2013 Jan-Mar; 3(1): 45–60.

[25] Baghaie A, Yu Z, D'Souza RM. "State-of-the-art in retinal optical coherence tomography image analysis." Quant Imaging Med Surg 2015;5(4):603-617. doi: 10.3978/j.issn.2223-4292.2015.07.02

Some of the specific techniques within these classifications include:

- Thresholding
- Clustering methods
- Motion and interactive segmentation
- Compression-based methods
- Histogram based methods
- Edge Detection
- Dual clustering method
- Region-growing methods
- Watershed transformation
- Model-based segmentation
- Multi-scale segmentation
- Semi-automatic segmentation
- Graph partitioning methods
- Variation methods
- Partial differential equation-based methods
- Fuzzy Histogram Hyperbolization (FHH)
- Contour Detection
- Hough Transform

By no means is this an exhaustive list but it illustrates the growth within the subject area.

Some image segmentation techniques/algorithms are more popular than others for OCT image scans where greater success is seen in the segments created with distinguishable layers, features, and abnormalities. These commonly used image segmentation techniques and algorithms are introduced in the next few subsections.

3.1 Edge Detection

Across all automated segmentation algorithms, edge detection is considered an essential foundation in accurate edge detection of the retinal layers in OCT image scans[26]. There are two main operators of edge detection algorithms, 1) gaussian based, 2) gradient based. Gaussian based includes canny edge detector, and Laplacian of gaussian. Gradient based includes Sobel operator, Prewitt operator, and Roberts operator.

Su Luo et al.[27] note one of the three most promising edge detection algorithms identified in related literature and include Canny Edge Detection in delineating the retinal layer boundaries in the OCT image scans.

[26] Q. Yang, C. A. Reisman, and Z. Wang, “Automated layer segmentation of macular OCT image scanss using dual-scale gradient information,” Optics Express, vol. 18, no. 20, pp. 21293–21307, 2010.
[27] Su Luo, Jing Yang, Qian Gao, Sheng Zhou, Chang’an A. Zhan, "The Edge Detectors Suitable for Retinal OCT Image Segmentation", Journal of Healthcare Engineering, vol. 2017, Article ID 3978410, 13 pages, 2017. https://doi.org/10.1155/2017/3978410

Canny Edge Detection is probably one of the most widely used algorithms. It was proposed by John Canny in 1986. It is a four step algorithm[28] and the steps include:

- The first stage removes the background noise in the image using a Gaussian filter so that the algorithm detects real edges
- The second stage computes the intensity gradient in the image using a Sobel filter (using a combination of Sobel-x and Sobel-y)
- In the third stage unwanted pixels are removed/suppressed so they will not be confused as edges. To do this, the entire image is analysed, checking if each pixel is a local maximum in the direction of the gradient relative to its area.
- Finally, the last stage is the application of the Hysteresis Thresholding. In this final stage the algorithm determines which edges are real edges and those which are not. It connects the broken edges. For this, two threshold values must be determined, the minVal the minimum threshold, and maxVal the maximum threshold. Any edge with an intensity gradient greater than maxVal will be an edge, and a value less than minVal will be discarded.

3.2 Clustering - K-Means

Clustering algorithms in machine learning are unsupervised algorithms that support classification. According to KDnuggets,[29] "in clustering, typically you do not know what you are looking for and are trying to identify some clusters in your data. K-Means clustering algorithm is used to segment the areas of interest from the background. It clusters the given data into K-clusters or parts based on the K-centroids. This algorithm is used with unlabelled data that does not have defined categories/groups/target labels. Ultimately, the goal of the algorithm is to find certain groups based on similarity in the data with the number of groups represented by K." As a result, K-Means clustering technique/algorithm is a popular method of image segmentation.

Cited from KDnuggets[30], the steps in "K-Means algorithm include:

- Choose the number of clusters K.
- Select at random K points, the centroids(not necessarily from your dataset).
- Assign each data point to the closest centroid → that forms K clusters.
- Compute and place the new centroid of each cluster.
- Reassign each data point to the new closest centroid. If any reassignment took place, go to step 4, otherwise, the model is ready."

[28] Source: https://dontrepeatyourself.org/post/edge-and-contour-detection-with-opencv-and-python/

[29] Nagesh Singh Chauhan, "Introduction to Image Segmentation with K-Means clustering", KDnuggets on August 9, 2019, https://www.kdnuggets.com/2019/08/introduction-image-segmentation-k-means-clustering.html

[30] Nagesh Singh Chauhan, "Introduction to Image Segmentation with K-Means clustering", KDnuggets on August 9, 2019, https://www.kdnuggets.com/2019/08/introduction-image-segmentation-k-means-clustering.html

The actual selection of K is ambiguous, this can be set to any value based on prior knowledge of data, shapes, colours etc. A value must be selected however in order to use the algorithm.

3.3 Thresholding

Shapiro et al. [31], state this method of image segmentation has been called "the simplest method. From a grayscale image, thresholding can be used to create a binary image". The key to this method is to select the threshold value (or values when multiple levels are selected) that are above a specific intensity level.

An overview of some of these thresholding techniques are below.

- Simple Thresholding: For every pixel, the same threshold value is applied. If the pixel value is smaller than the threshold, it is set to 0, otherwise it is set to a maximum value.

- Adaptive Thresholding: Adaptive thresholding is the method where the threshold value is calculated for smaller regions and therefore, there will be different threshold values for different regions[32].

- Otsu's Binarization: Otsu's thresholding method involves iterating through all the possible threshold values and calculating a measure of spread for the pixel levels each side of the threshold, i.e., the pixels that either fall in foreground or background[33].

3.4 Contour Detection

Contour detection is mainly used to determine the shape of closed objects. OpenCV[34] states "contours are simply a curve joining the continuous points along the boundary having the same colour intensity. Contour detection is a useful method for shape analysis in object detection and recognition of what is inside an image".

A frequently asked question is how contour detection differs from edge detection as both are used for determining the shape of an object. In the simplest terms, according to Rama, 2020[35] "edge detection is carried out for the whole image whereas contour detection is carried out only for the

[31] Shapiro, Linda G. & Stockman, George C. (2002). "Computer Vision". Prentice Hall. ISBN 0-13-030796-3

[32] OpenCV- Adaptive Thresholding, https://www.tutorialspoint.com/opencv/opencv_adaptive_threshold.htm#:~:text=Adaptive%20thresholding%20is%20the%20method,()%20of%20the%20Imgproc%20class

[33] Sunil L. Bangare, Amruta Dubal , Pallavi S. Bangare ,Dr. S. T. Patil, "Reviewing Otsu's Method For Image Thresholding",International Journal of Applied Engineering Research, ISSN 0973-4562 Volume 10, Number 9 (2015) pp. 21777-21783

[34] OpenCV, source: https://docs.opencv.org/3.4/d4/d73/tutorial_py_contours_begin.html

[35] Tejas Rama, "Contour Detection & Edge Detectuib with opencv", Medium, Juk 19, 2020. Source: https://medium.com/@tejas9723/contour-detection-edge-detection-with-opencv-96a74097e1f6

objects in the image". The level of detail in a contour image will not be as granular as the edge detection as only boundaries of the objects are identified.

For objects within an image, contour hierarchies help denote the parent-child relationship between contours. The contour-retrieval mode used affects contour detection in images, and produces these hierarchical results. Parent-Child relationships can be established for single objects scattered around in an image, or objects and shapes inside one another[36].

3.5 Texture Segments

Madasu et al., define "texture segmentation is the process of partitioning an image into regions with different textures containing similar group of pixels"[37]. Texture is the main term used to define objects or concepts of a given image. Texture analysis methods usually are grouped into four categories: statistical methods, structural, model-based, and transform-based methods according to Armi, et. al[38]. An overview of these methods has been provided below cited from Armi, et. al "Texture image analysis and texture classification methods - A review".

> Statistical Methods: This set of methods "analysing the texture of images perform a series of statistical calculations on the lightness intensity distribution functions of pixels. The methods are used to derive feature vectors from statistical computations. The first- level single-pixel specification is calculated without taking into account the interaction between pixels of the image. While in a second-level and higher- level statistical characteristic, the specification is calculated taking into account the dependence of two or more pixels. The Co-Occurrence Matrix that is known as the second-level histogram is one of the methods to be included in this group."

> Structural Methods: For this set of methods, "the texture is introduced based on the initial units and their spatial layout. Initial units are a pixel, a region, or a line-like shape. The structural methods consider texture as a combination of initial patterns, once the primary texture is detected, and then the statistical properties of the primary texture are calculated, and used as a feature."

> Model-Based Methods: The model-based method is used for texture modelling, and "the most popular ones are Autoregressive (AR) method, Markov Square theory, Gibbs RMF, Hidden Markov Model(HMM), and fractal model. A model of the image is created and then this model is used to describe the image synthesis. Model parameters extract the basic

[36] Source: https://learnopencv.com/contour-detection-using-opencv-python-c/

[37] Vamsi Krishna Madasu, Prasad Yarlagadda, "An in Depth Comparison of Four Texture Segmentation Methods," 9th Biennial Conference of the Australian Pattern Recognition Society on Digital Image Computing Techniques and Applications (DICTA 2007), 2007, pp. 366-372, doi: 10.1109/DICTA.2007.4426820.

[38] Laleh Armi, Shervan Fekri-Ershad, "Texture image analysis and texture classification methods - A review", International Online Journal of Image Processing and Pattern Recognition, Vol. 2, No.1, pp. 1-29, 2019

qualitative properties of the texture. A fractal geometric model is a model used to analyse many natural and physical phenomena."

Transform-based Methods: With this set of methods, "the image is transformed into another space, so that the texture is more easily distinguishable in the new space. The most used extraction methods in this method are Wavelet transforms, Curvelet, Ridgelet and Gabor."

3.6 Nuclei Analysis Using Watershed

The watershed algorithm extracts the sure background and foreground and then leveraging markers will make watershed run and detect the exact boundaries. Markers can be user defined manually or using a defined algorithm such as thresholding or morphological operations. Generally, the algorithm helps in detecting touching and overlapping objects in image[39].

According to Wikipedia[40], the watershed transformation considers the gradient magnitude of an image as a topographic surface. Pixels having the highest gradient magnitude intensities (GMIs) correspond to watershed lines, which represent the region boundaries. Water placed on any pixel enclosed by a common watershed line flows downhill to a common local intensity minimum (LIM). Pixels draining to a common minimum form a catch basin, which represents a segment.

Aegis[41] notes the steps for image segmentation using watershed algorithm as:

- Finding the sure background using morphological operations like opening and dilation.
- Finding the sure foreground using distance transform.
- Unknown area is the area neither lies in foreground and background and used it as a marker for watershed algorithm

3.7 Blob Detection

Blob detection is another popular technique/algorithm. Caubalejo[42] defines this as:

"a blob is anything that is considered a large object or anything bright in a dark background, in images, we can generalise it as a group of pixel values, that forms a colony or a large object that is distinguishable from its background. Using image processing, we can detect such blobs in an image."

Pre-processing steps for blob detection include binarization as it is easier to work with the smaller dimensions and normalised values. Binarization methods use a threshold on the pixel value where there is a separation within this value.

---

[39] Aegis, "Watershed Algorithm and its application for image segmentation", https://www.aegissofttech.com/articles/watershed-algorithm-and-limitations.html

[40] Source: https://en.wikipedia.org/wiki/Image_segmentation#Watershed_transformation

[41] Aegis, "Watershed Algorithm and its application for image segmentation:, https://www.aegissofttech.com/articles/watershed-algorithm-and-limitations.html

[42] Caubalejo, "Image Processing - Blob Detection", https://towardsdatascience.com/image-processing-blob-detection-204dc6428dd

There are different functions to use for circular blob detection which are[43]:

- Laplacian of Gaussian Method
- Difference of Gaussian(DOG)
- Determinant of Hessian (DOH)

3.8 Pre-Processing Techniques

As OCT image scans have a high level of speckle noise, some form of pre-processing methods are usually performed to reduce the effect of noise. In most cases, even though the segmentation algorithms are designed to handle noise, pre-processing is used as a first step to handling the noise according to a study by Dodo et al.[44]. The primary goal of noise reduction is to remove the noise without losing much detail contained in the image.

In general, results of the original unprocessed image can be improved by some of the following pre-processing techniques:

- Increasing resolution
- Deskewing the image
- Blurring of the image
- Convert to black and white
- Remove noise through operations like morphological transformation, contours etc.

These techniques should be tested on the OCT data to see which produce the best results.

4. Methodology for Dissertation

4.1 Outline of Steps

This section explains the methodology that will be followed for the data analysis of this study. It will provide insights into the level of accuracy, completeness, reliability, and relevance with all steps taken. An overview has been provided in figure 9.

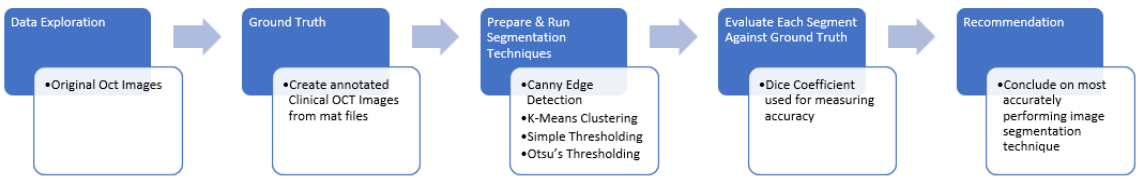

[43] Caubalejo, "Image Processing - Blob Detection", https://towardsdatascience.com/image-processing-blob-detection-204dc6428dd

[44] Bashir Isa Dodo, Yongmin Li, Khalid Eltayef & Xiaohui Liu, "Automatic Annotation of Retinal Layers in Optical Coherence Tomography Images", Journal of Medical Systems, Published: 13 November 2019

Figure 9: Outline for methodology

The methodology is closely linked to Cross Industry Standard Process for Data Mining (CRISP-DM) which is the most common methodology for data mining, analytics, and data science projects. Ensuring there is business understanding, data understanding and preparation, modelling, and evaluation from CRISP-DM.

The image segmentation techniques/algorithms being used to analyse the OCT scans are:

- Canny Edge Detection
- K-Means Clustering
- Simple Thresholding
- Otsu's Thresholding

In total, 25 unprocessed original images and their annotated ground truth images will be used creating an initial dataset of 50 images for this analysis. As shown in figure 10, the 25 combined unprocessed original images, will be used to create segmented images leveraging each of the 4 image segmentation techniques/algorithms.

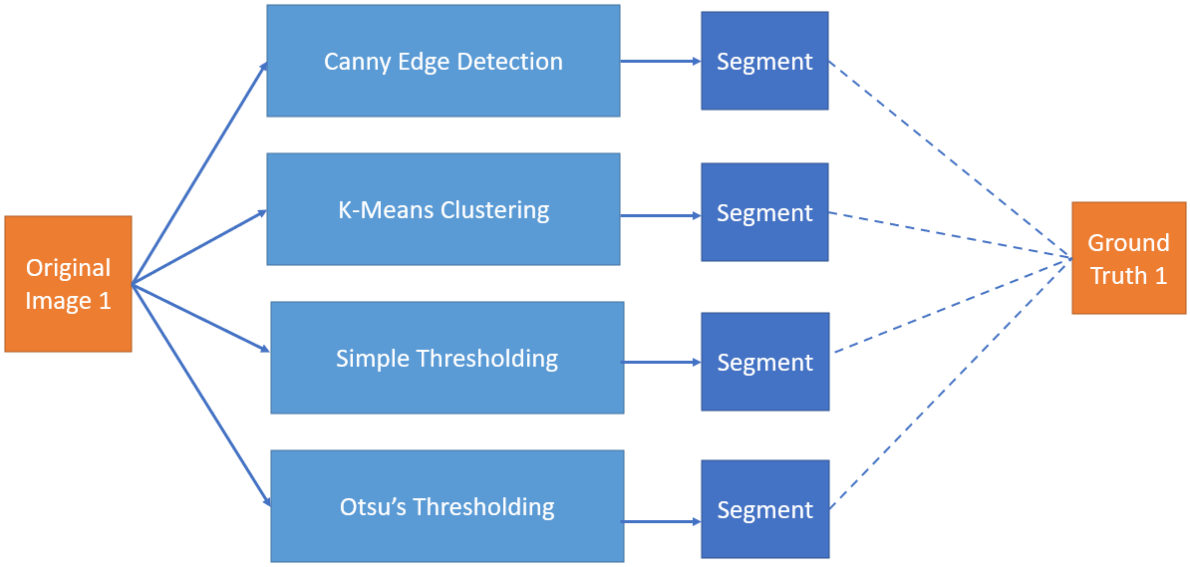

Figure 10: Overall approach of how an original image will be used to create new segmented images. Dotted line represents comparison of new segmented images to ground truth.

Each segmented image will then be compared to the corresponding ground truth for accuracy using an evaluation metric. With the additional segmented images that are created, this will take the total final dataset to 150 images. All these images will be submitted with this dissertation.

4.2 Evaluation Metric: Dice Coefficient

For the quantitative analysis of this study, the dice coefficient value will be leveraged to evaluate accuracy of each image segmentation technique/algorithm. It compares the pixel-wise agreement

between the new segmented image from image segmentation algorithm which has all the discovered retinal layers present and the corresponding clinically annotated ground truth. It is a measure of the overlap between the two. Should the value be 1, it indicates a perfect overlap, while 0 indicates no overlap between the two images – as shown in figure 11.

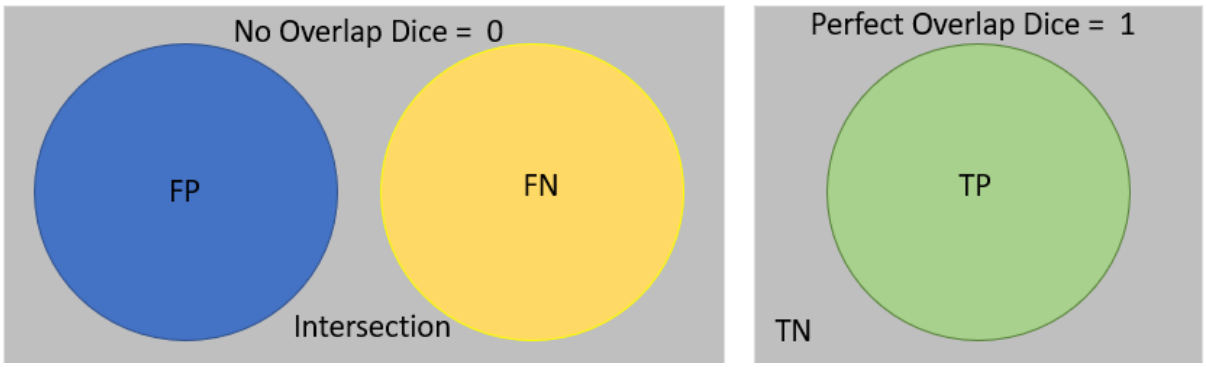

Figure 11: Overlapping and non-overlapping images

This method will assist with understanding the accuracy of the segmented images. The average of the dice coefficient from across each image segmentation techniques/algorithms will be used in the final conclusion.

In the upcoming sections, the steps involved will be explained, some examples shown of the ground truth image and the segmented images for the specific segmentation techniques/algorithms.

4.3 Programming Language

Python is the main programming language that will be used. Images will be read using skimage or OpenCV packages. Processing of images will use skimage, OpenCV, Glob, Shutil, OS packages; processing on multidimensional data will useNumPy and SciPy packages; for dataframes Pandas package will be used. Other libraries included matplotlib for plotting.

5. Data Exploration

The dataset used for the dissertation study came from Optical Coherence Tomography Image Retinal Database shared by a study from Gholami, et al., 2018[45]. Manual Segmentation folder[46] from this database includes a number of image pairs. These pairs include the unprocessed original image (jpeg format) along with the corresponding ground truth delineation (raw data, no jpeg and provided in mat file format). The ground truth data has been determined by an expert. To provide an overview of the OCT data, some characteristics have been explored to gain a basic understanding.

[45] Peyman Gholami, Priyanka Roy, Mohana Kuppuswamy Parthasarathy, Vasudevan Lakshminarayanan, "OCTID: Optical Coherence Tomography Image Database", arXiv preprint arXiv:1812.07056, (2018).
[46] For more information and details about the database see: https://arxiv.org/abs/1812.07056

Each of the 25 unprocessed images in the dataset has dimensions of 924-pixel width, height of 616-pixels, and are a combination of colour and greyscale. Figures 12 and 13 shows the unprocessed original OCT image scans in colour and greyscale. There is a significant level of speckle noise in the OCT image scans which is reducing its quality and will impact the image segmentation techniques/algorithms ability to identify retinal layers, features, and abnormalities.

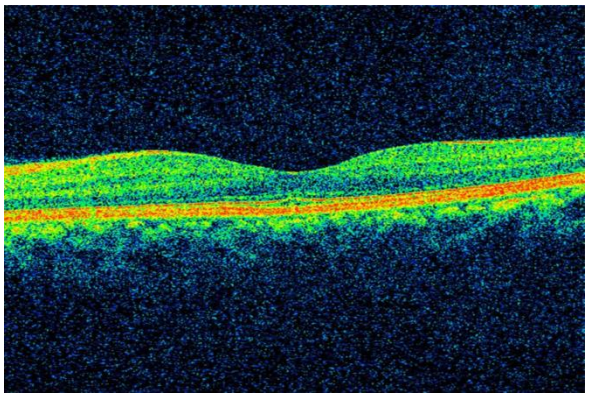
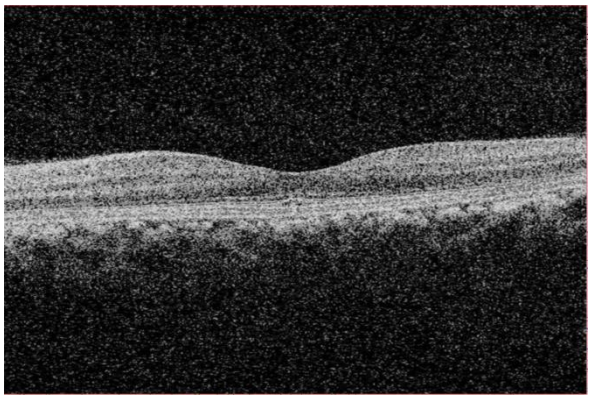

Figure 12: Colour Original OCT image scans; Figure 13: Greyscale Original OCT image scans

Figure 14 shows a manually segmented ground truth that was developed from the dataset that will be used for comparison in the dice calculation. The ground truth images display only the retinal layers from the OCT scan images and have noise entirely removed. This much simpler form of the scanned image makes it much easier to identify features and abnormalities easily assisting health condition diagnosis and monitoring.

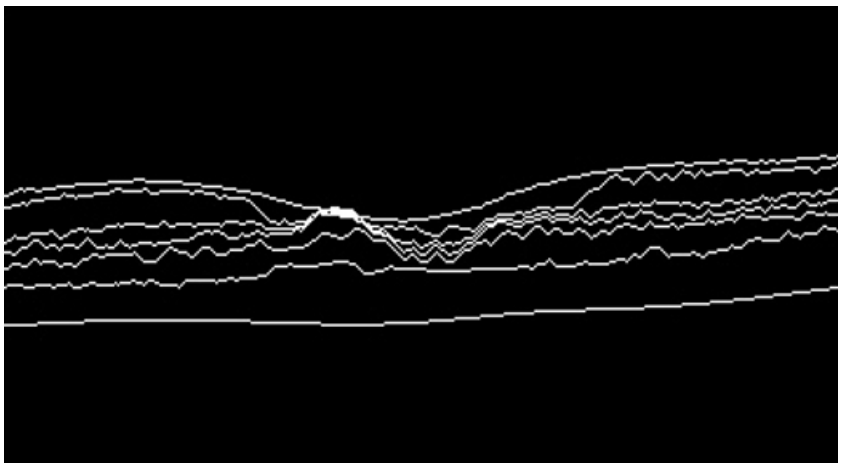

Figure 14: Ground Truth OCT image

To work with the OCT data in any form of analysis, it is important to see the structure of it numerically as this is how the programming library/packages, functions and algorithms that will be leveraged will work with the dataset.

The unprocessed images can be read in python using BGR (blue, green, red) colour space or greyscale depending on what the desired outcome is to be performed. The corresponding values can be displayed in an image matrix to understand the structure of the data. Figure 15 shows the first row of the image matrix in BGR colour space. In this unprocessed image, every pixel is represented by its B, G and R components. This is the default colour space in which images are read in OpenCV.

```
The first row of the image matrix contains 924 pixels
[[105  31   0]
 [ 86  20   0]
 [ 49   0   0]
 ...
 [ 78  25   4]
 [ 83  28   1]
 [ 82  28   0]]
```

Figure 15: First row of image matrix for original OCT in BRG

At times, depending on the action being performed, use of grayscale and/or floating-point numbers for the image are required to have it in a format that algorithms can work with. It also helps to continue to understand the structure of the image, figure 16 provides some of the first row's image matrix in greyscale using skimage package and as_gray=True function. This loaded the image in greyscale luminance of each pixel.

```
The first row of the image matrix contains 924 pixels
[0.13044706 0.07316235 0.01668196 0.01043961 0.05948078 0.19951647
 0.22554588 0.11465843 0.03295608 0.0131251  0.00763412 0.02953451
 0.0247498  0.03368706 0.05520745 0.04904667 0.08635843 0.06176471
 0.03625451 0.01465882 0.00706863 0.01425608 0.02151804 0.04525765
 0.05065255 0.09306157 0.09051686 0.06100431 0.09057529 0.13246078
 0.06299569 0.01461333 0.02700392 0.01270157 0.0399302  0.11461333
 0.16595176 0.13307451 0.02675098 0.00931569 0.00733647 0.00817765
 0.03679804 0.09519176 0.33281176 0.53595176 0.38747412 0.11383098
 0.10669647 0.10445647 0.07583608 0.03738549 0.01291686 0.02180078
 0.02150314 0.01453882 0.01038706 0.01378863 0.01602863 0.01855137
 0.01826863 0.02192235 0.02218235 0.01990471 0.1152898  0.13959216
 0.08405647 0.01596745 0.01324431 0.01555098 0.03129686 0.1202902
 0.15138863 0.14367137 0.06508314 0.00841647 0.00841647 0.04073451
 0.0901902  0.12953294 0.16482941 0.07555333 0.01715961 0.02382627
 0.02820824 0.00583333 0.00280549 0.01963843 0.04462706 0.01966039
 0.00452392 0.00706863 0.01831255 0.14155922 0.22689882 0.18870902
 0.08329765 0.04324863 0.01746431 0.01381059 0.01352784 0.01267961
 0.01070039 0.02725059 0.15045608 0.1179149  0.04170078 0.0025
 0.00083333 0.00141373 0.00591569 0.03622471 0.0946702  0.09184196
 0.07017882 0.03394549 0.02769373 0.0363098  0.03546157 0.0287651
 0.01343765 0.00537216 0.00902588 0.0466502  0.03823373 0.02196627
 0.01720353 0.01102706 0.01154863 0.01378863 0.05869843 0.11421922
```

Figure 16: Start of first row of image matrix for original OCT in greyscale and floating-point values

Therefore, the three red, green, and blue (RGB) values are combined into a single value when removing colour from an image. Luminance can also be described as brightness or intensity, which can be measured on a scale from black (zero intensity) to white (full intensity).

5.1 Pre-Processing

Various techniques were attempted to pre-process the unprocessed OCT image scans dataset to remove some noise and improve image quality before running the finalised set of image segmentation techniques/algorithms. Below are examples of those that were attempted.

Rescaling and resizing failed to show any improvements to image quality or noise reduction. Resizing appeared to have reduced the quality of the OCT image scans compressing the level of detail and no benefit being driven.

Filter functions were also tested using Gaussian and Sobel on the original OCT image scans dataset. With Gaussian (figure 17) the level of detail for the retinal layers became somewhat diminished. With Sobel (figure 18), the speckle noise seems to have worsened as well as poor quality of the retinal layers. No success discovered from either of these techniques.

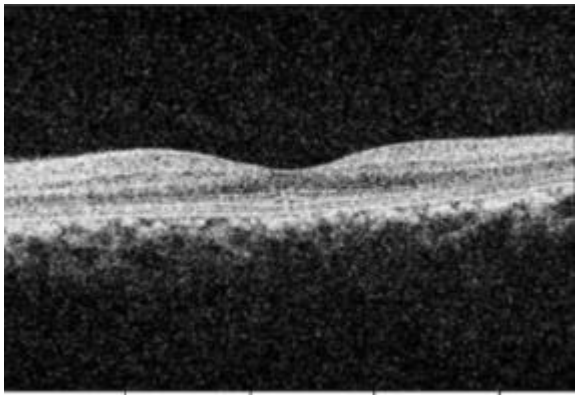

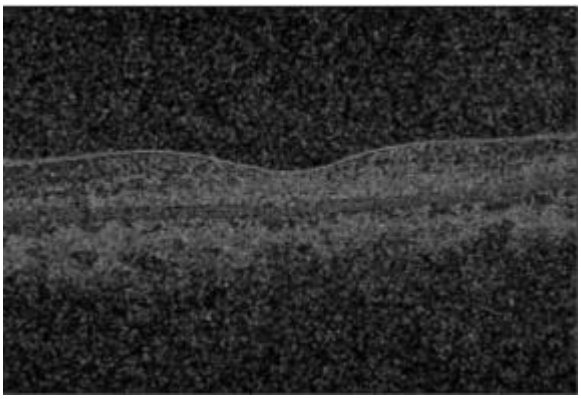

Figure 17: Gaussian filter on original OCT image scans; Figure 18: Sobel filter on original OCT image scans

From research, it has been found that the median filter is typically used to denoise, being the most successful with OCT image scans. The median filter was leveraged using skimage and a kernel size of 3 was used – see figure 19 for the results. It's clear with this dataset minimal noise appears to have been removed and slightly blurred the quality; overall it is not much of an improvement to the original OCT scan.

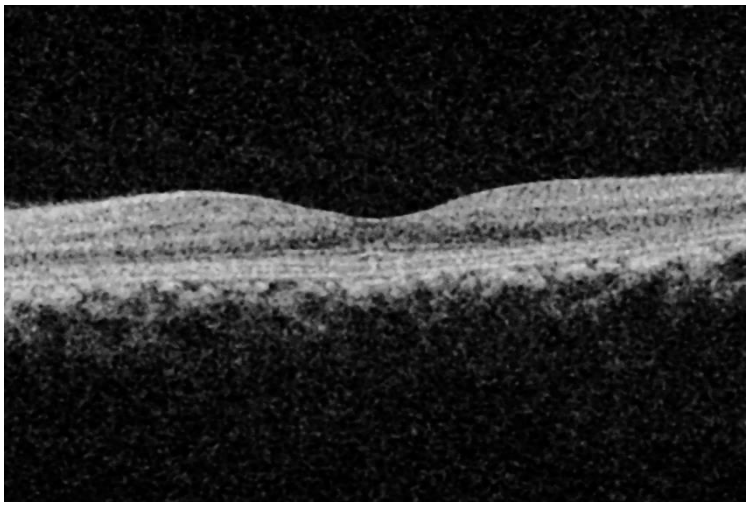

Figure 19: Median filter on unprocessed/original OCT image scans using skimage

The decision was made to move forward with no pre-processing of the dataset due to limited success with image quality improvement. Should a segmentation technique/algorithm require pre-processing as part of the method, it will be leveraged and will be specifically called out when performed.

6. Ground Truth

The ground truth images as mentioned, come from Optical Coherence Tomography Image Retinal Database[47]. The dataset provided Mat files which contained details of the retinal layers that were annotated by an expert for each of the 25 images. For each image, there were 7 retinal layers identified – this included the names of each layer together with the x and y coordinates to be able to plot these to compile the whole annotated OCT image scan.

For reference, a sample of the compiled ground truth images have been provided below together with the corresponding original unprocessed image for a comparison of the changes that take place when a clinical professional manually annotates the images. See figures 20 to 25.

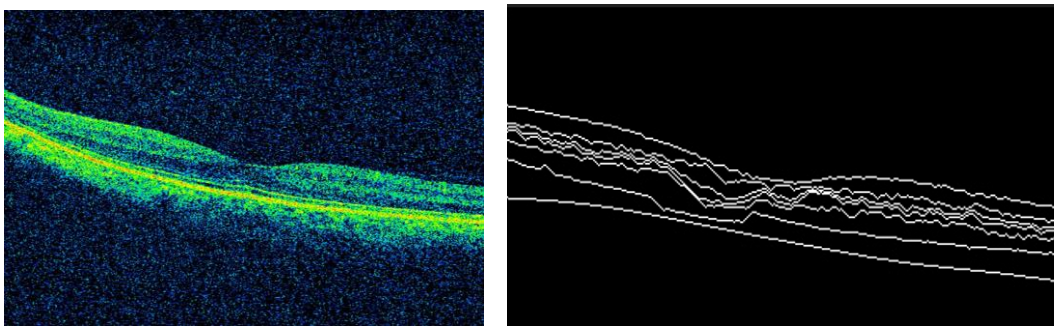

Figure 20: Unprocessed Image 10 Macula; Figure 21: Ground Truth of Image 10 Macula

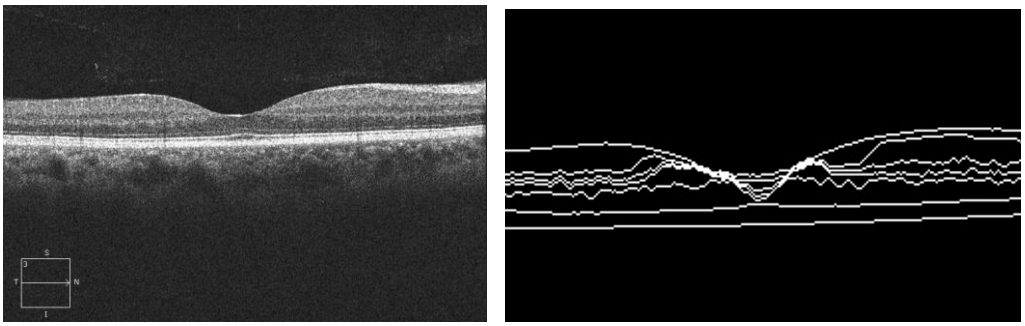

Figure 22: Unprocessed Image 22 OD; Figure 23: Ground Truth of Image 22 OD

[47] Peyman Gholami, Priyanka Roy, Mohana Kuppuswamy Parthasarathy, Vasudevan Lakshminarayanan, "OCTID: Optical Coherence Tomography Image Database", arXiv preprint arXiv:1812.07056, (2018).

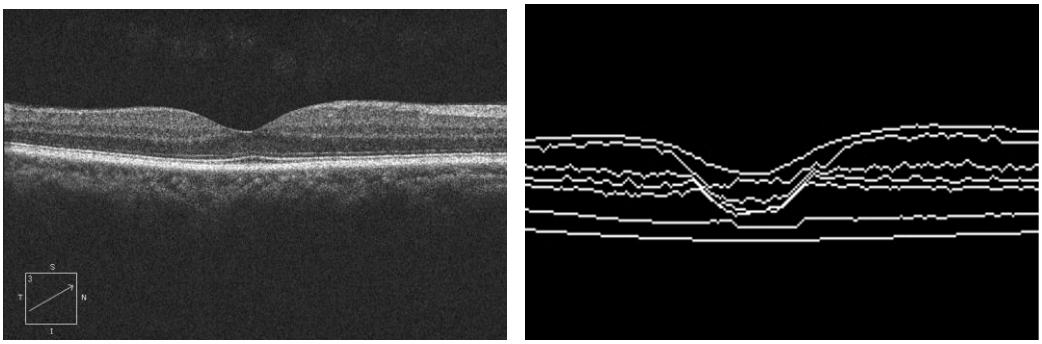

Figure 24: Unprocessed Image 108 OD; Figure 25: Ground Truth of Image 108 OD

As can be seen, the ground truth images are black and white. The white lines on the black background represent the lines of the 7 retinal layers. All noise has been removed from the image. The layers easily show features and abnormalities that are difficult to see in the unprocessed image. The ground truth is a simpler version with less complexity, it helps the eye to focus on the critical areas including retinal layer thickness being visible.

Of all 25 ground truth images, each are different to one another based on the original unprocessed image - of the examples provided above this can be clearly seen. The commonality across all ground truths is that the complexity from the image is removed showing just pertinent information for the ophthalmologist to focus on.

For this dissertation study, the segmented images will be compared to the corresponding ground truths and accuracy of the algorithm evaluated using the dice coefficient metric.

7. Comparison/Image Segmentation Techniques

7.1 Segmentation Technique 1: Canny Edge Detection

7.1.1 Why the Technique Was Selected

An overview of the Canny Edge Detection algorithm and the steps involved have been explained in detail in section 3.1. This technique was leveraged as it is considered the 'standard' in OCT image segmentation. It is known to be one of the best in delineating the retinal layer boundaries in OCT image scans. Thus, providing a good opportunity for high-quality segmented images to be produced.

7.1.2 How the Technique Works

The algorithm steps for Canny Edge Detection have been described in detail in section 3.1. Please note, this does include applying the median filter for blurring as part of the algorithm to prepare the data.

In running the segmentation technique/algorithm, OpenCV was used for this technique, following each 4 steps of the algorithm. Converting the images to greyscale, applying the Gaussian blurring function (5, 5 as the kernel size), and then the Canny function.

7.1.3 Segmented Results & Parameters Leveraged in Technique

Figure 26 shows one of the segmented image that were created by the Canny Edge Detection technique/algorithm. It has produced a simplified image with significant speckle noise being reduced and some retinal layer boundaries identified.

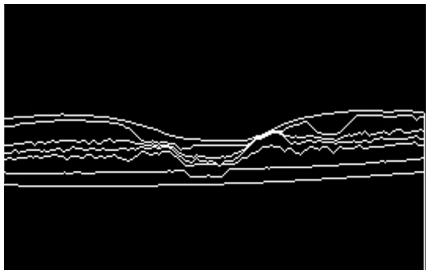

Figure 26: Canny Edge Detection Segmented Image from 06 OS; Figure 27: Ground Truth Image 06 OS

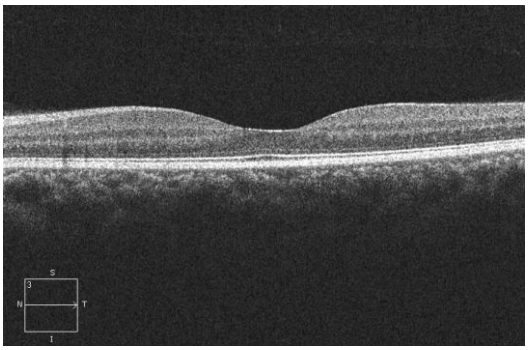

Figure 28: Original Unprocessed Image 06 OS

Figure 26, the Canny Edge Detection segmented image, shows 3 clear retinal layers and a partial 4th layer, however there are three layers which the algorithm has entirely missed. The missing three retinal layers could be where some edges have been detected although they are not a persistent continuous line from left to right. When referencing figure 27, the ground truth, figure 26 does appear to have edges detected corresponding to where figure 27 has retinal layers annotated.

Upon review of the segmented image to the ground truth (figure 27), it's clear to see which layers are missing. This will impact the dice coefficient score which calculates the pixel-wise agreement between the 2 images.

In comparing the segmented image to figure 28, the original unprocessed image, some detail within the image has been lost although the noise is significantly reduced. The algorithm has been successful in creating a simplified segmented image.

To produce these segmented results, specific parameters were set and adjusted to see which values produced less noisy images with a greater number of retinal layers present for Canny Edge Detection. The final parameters used were:

- Gaussian Blur with kernels 5, 5
- Canny with thresholds 150, 175

These parameters enabled the algorithm to create segmented images where the majority (20 out of 25 segmented images) were without noise and had clear distinguishable layers. They looked similar to the ground truth type of image.

Other parameters that were tested but did not produce successful segmented images included:

- Gaussian Blur with Kernels of 3, 3; 2, 2; Canny with thresholds 75,100; 50,100; 100, 175
- Gaussian Blur with Kernels of 5, 5; Canny with thresholds 75,100; 50,100

The attempts created segmented images that detected vast amounts of noise and the Gaussian blur method did not seem to have worked as well. Both figures 29 and 30 show a significant amount of noise above and below the middle area where retinal layers are present, and it's difficult to distinguish the retinal layers. Please note, this is a non-clinical expert professional direct observation and own judgement was used. These were not selected as the final parameters to proceed forward with.

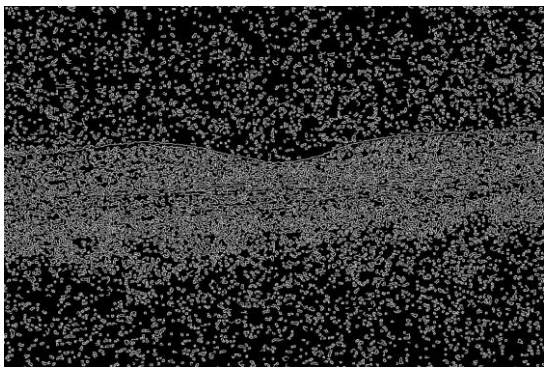

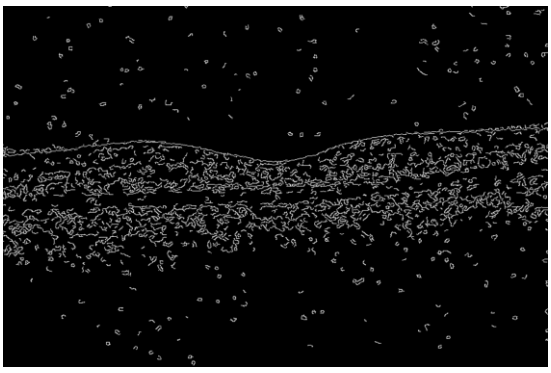

Figure 29: Kernel size of 3, 3, and Canny thresholds of 100 and 175; Figure 30: Kernel size of 5,5 and Canny thresholds of 100, 175

All 25 canny segmented images were then prepared and compared to their corresponding ground truths.

7.1.4 Evaluation: Dice Coefficient

Leveraging each Canny Edge Detection segmented image and comparing them to the corresponding ground truths, supported the dice coefficient to be calculated to evaluate the accuracy of the image segmentation technique/algorithm. Each dice score was saved in a Pandas data frame and exported into excel, the output is shown in table 1.

Segmented Image Number	Canny Edge Dice Coefficient
1	0.649
2	0.281
3	0.686
4	0.65
5	0.714
6	0.731
7	0.653
8	0.841
9	0.317
10	0.657
11	0.641
12	0.287
13	0.726
14	0.668
15	0.792
16	0.308
17	0.672
18	0.661
19	0.612
20	0.671
21	0.676
22	0.679
23	0.297
24	0.634
25	0.285
AVG	**0.592**

Table 1: Canny Edge Detection Segmentation Dice Coefficients and Average

As mentioned in section 4.2, dice coefficient measures the overlap between the segmented image and the clinically annotated ground truth. Specifically comparing the pixel-wise agreement. In recap, the score provides a value between 1, to indicate a perfect overlap, or 0 indicating no overlap between the two images. Table 1 shows fairly high dice coefficient values indicating they have a reasonable overlap across the dataset. As mentioned above, through direct observation Canny Edge Detection did detect close to 4 retinal layers, and potentially several edges detected where the ground has retinal layers annotated in those areas, which aligns well with the data in table 1.

There is one segment (number 8) that aligns particularly well with the ground truth with a 0.84 dice coefficient. Figure 32 displays segmented image number 8 from table 1, and when compared to figure 31, the ground truth, it has detected many edges although not all are persistent continuous lines from left to right. Only one retinal layer is detected with a continuous line. The edges on figure 32 do align with where annotated retinal layers exist on figure 31. Overall, despite having the highest dice coefficient score, it is clear (to a non-clinical expert) to see complexity with the edges and not a

more simplified image as desired. However, to a clinical expert, they may be able to detect the retinal layers and abnormalities more clearly from the edges identified by Canny Edge Detection.

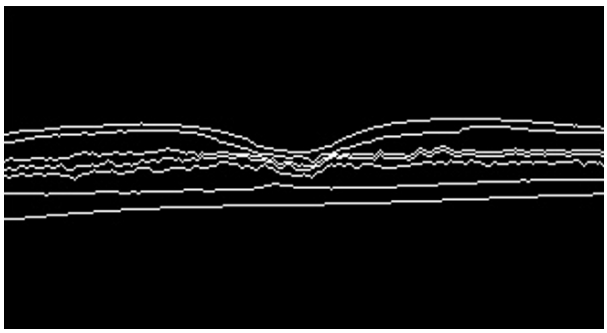

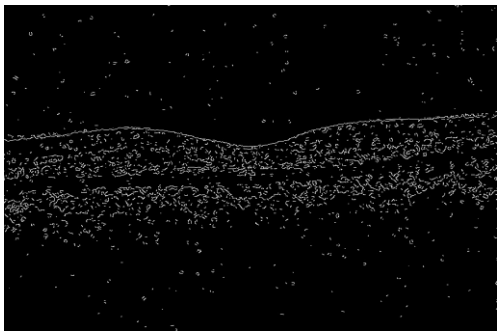

Figure 31: Ground Truth Image 198 OS; Figure 32: Canny Edge Detection Segmented Image 198 OS

It is important to note however, none of the Canny Edge Detection segmented images are perfectly overlapping as an exact match with the ground truth.

Also displayed in table 1, is the average dice coefficient for Canny Edge Detection image segmentation algorithm. It is important to review this as a single value of the algorithm's performance. At 0.592, it indicates a promising image segmentation algorithm for this dataset. Canny Edge Detection algorithm's ability to detect the retinal layers, features, and abnormalities in the same way as the clinically annotated ground truth is fairly good - promising even. In addition, its ability to remove noise and simplify the image seems to have worked well with this dataset. There is a good level of overlapping across both sets of images at the intersection points. Given how the algorithm works (each of the 4 steps) and is calculated, it is easy to see why there would be some level of success with this method. As mentioned in an earlier section, this algorithm is considered the essential foundation to edge detection of retinal layers and can be witnessed with the high performance.

7.2 Segmentation Technique 2: K-Means Clustering

7.2.1 Why the Technique Was Selected

K-Means Clustering is an unsupervised machine learning algorithm to segment different parts of an image. Clustering is a key image segmentation method and offers variety in the dissertation study results across all the techniques leveraged.

7.2.2 How the Technique Works

K-Means clustering algorithm aims to partition N observations into K clusters in which each observation belongs to the cluster with the nearest mean[48]. A cluster refers to a collection of data points aggregated together because of certain similarities. For image segmentation, clusters here are different image colours.

The objective of K-Means clustering is to minimise the sum of squared distances between all points and the cluster center[49]. The formula is displayed in figure 33.

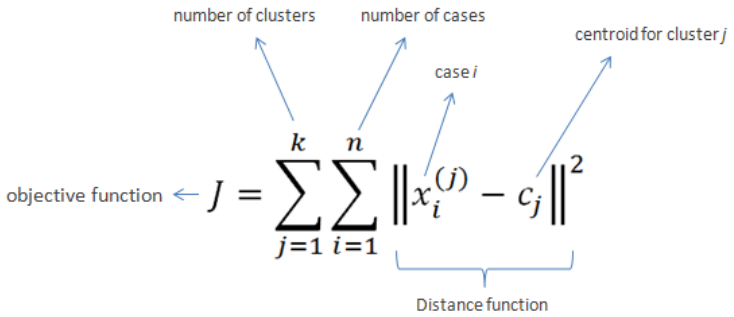

Figure 33: Image Source: saedsayad.com

The K-Means Clustering unsupervised machine learning algorithm used was from OpenCV. Other libraries leveraged include NumPy and scikit-image. In the process, a median filter was applied, the image converted from BRG to RBG with the OpenCV COLOR_BGR2RGB function, a kernel size of 3 was applied leveraging cv.KMEANS_RANDOM_CENTERS function.

7.2.3 Segmented Results & Parameters Leveraged in Technique

Figure 34 shows one of the segmented images created using the K-Means clustering technique/algorithm. With how this algorithm works, it has leveraged K=3, therefore has 3 colour values displayed for the boundaries it has found. There appears to be no noise present at the top or bottom of the image in its attempt to simplify the unprocessed image. But due to the way in which clusters are identified, it still is a fairly complex image. The retinal layers are not thin lines but thick retinal areas representing the entire layer in colour.

[48] Sourodip Kundu, "KMeans For Beginner", Median on Nov 4, 2019. Source: https://medium.com/@KunduSourodip/kmeans-for-beginner-4af96166379e

[49] Nagesh Singh Chauhan, "Introduction to Image Segmentation with K-Means clustering", KDnuggets on August 9, 2019, https://www.kdnuggets.com/2019/08/introduction-image-segmentation-k-means-clustering.html

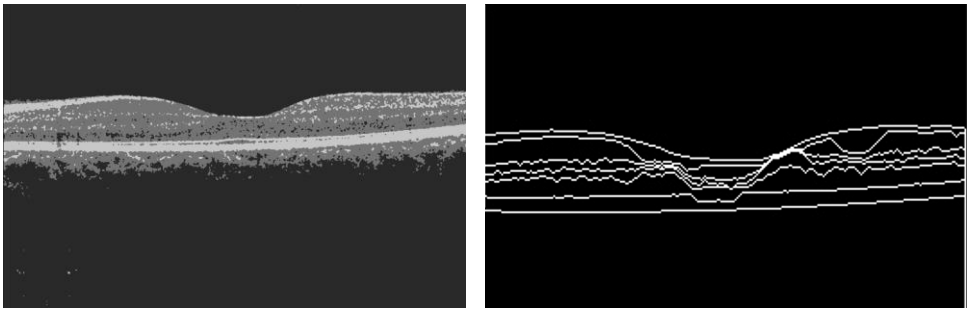

Figure 34: K-Means Clustering Segmented Image from 06 OS; Figure 27: Ground Truth Image 06 OS

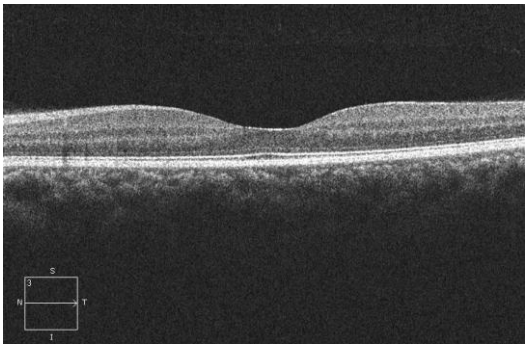

Figure 28: Original Unprocessed Image 06 OS

In comparing figure 34 with figure 27, the ground truth, we can distinguish approximately 4 retinal layers that the K-Means algorithm found which is where most of the coloured layers are persistent from across left to right. Where there the smaller clusters in lighter colour on figure 34 exist on the K-Means segmented image, they appear to align with where some of the annotated layers on figure 27. Overall, the style of the K-Means segmented image is very different to the ground truth image. The algorithm does not identify all the retinal layers as clearly as the ground truth.

Figure 34 is still much clearer and less complex than figure 28 which is the original unprocessed image. The K-Means Clustering algorithm has been somewhat successful to identify retinal layers, features, and abnormalities. A professional clinical expert will be able to confirm the extent of this, but these are assumptions being drawn based on direct observation.

For this segmentation algorithm, a cluster size of K = 3 was used as the optimal to see the greatest level of detail before most of the quality was lost. The success seen with the K = 3 parameter varied across each of the 25 unprocessed images as all OCT images are different including their quality. In total 6 of the 25 segmented images still showed significant speckle noise but 19 images showed substantial noise reduction and retinal layers that were distinguishable.

Other parameters were attempted but unfortunately the segmented images created did not produce as successful results. These attempts included cluster K:

- 2
- 4
- 5
- 6

Figures 35 and 36 show some of these attempts and the issues faced. Figure 35 with kernel size of 6, shows the speckle noise did not reduce, and the 6 colours used for the clusters are difficult to distinguish between them. Figure 36 has a kernel size of 2 and the level of detail appears to have been diminished. The 2 colours leveraged by the algorithm have caused the classification of all retinal layers in one colour. The quality of the segmented images using these parameters are reduced and therefore were not used in the final parameter set.

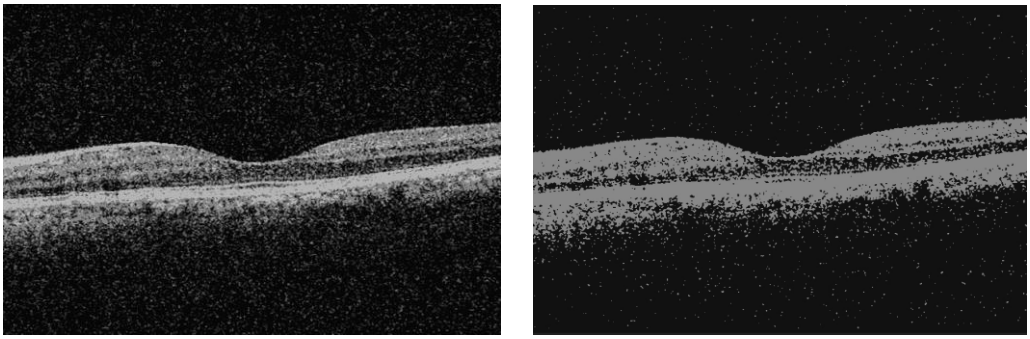

Figure 35:Kernel size of 6; Figure 36: Kernel size of 2

Using K = 3, all 25 K-Means cluster segmented images were then prepared for the next step of analysis.

7.2.4 Evaluation: Dice Coefficient

For each K-Means Clustering segmented image, the dice coefficient was calculated to evaluate accuracy of the algorithm against the corresponding ground truths. The individual dice coefficient values and an average have been provided in table 2.

Segment Image Number	K Means Dice Coefficient
1	0.046
2	0.064
3	0.045
4	0.043
5	0.045
6	0.045
7	0.043
8	0.055
9	0.059
10	0.045
11	0.045

12	0.06
13	0.049
14	0.045
15	0.054
16	0.065
17	0.044
18	0.045
19	0.042
20	0.043
21	0.044
22	0.043
23	0.07
24	0.044
25	0.062
AVG	**0.05**

Table 2: K-Means Clustering Segmentation Dice Coefficients and Average

The dice coefficient values returned are extremely low indicating very limited overlapping of K-Means Clustering segmented images to its corresponding ground truth. There is minimal intersection between them. This could be due to how the algorithm does its classification. Instead of showing the thinner lines for the retinal layer boundaries, it shades the entire retinal layer causing pixel to pixel agreement in the comparison to be off.

The highest dice coefficient score obtained is 0.07 (segmented image number 23) which is still significantly low. As can be seen in figures 37 and 38 below, despite having the largest dice coefficient score of the K-Means Clustering algorithm, there is a great difference across both images. The segmented image may have detected some of the retinal layers matching on the pixels of lines in the ground truth, but they are not as clear to distinguish as the ground truth. Also, the value is still low at 0.07 because of the vast differences between the segmented image to the ground truth – the speckle noise, the whole areas of retinal layers etc.

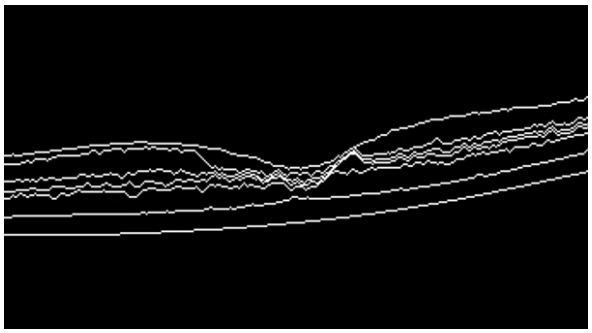

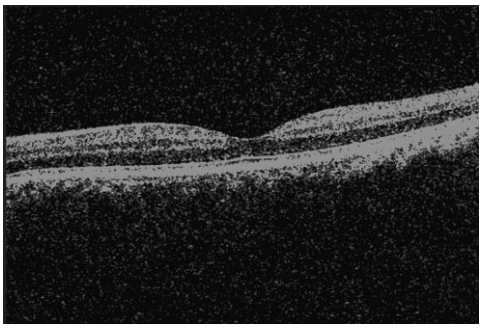

Figure 37: Ground Truth 8 macula; Figure 38: K-Means Clustering Segmented Image Number 23 (8 macula)

The average dice coefficient for the K-Means Clustering algorithm is 0.05, confirming that this type of algorithm was not suited to this dataset. As mentioned previously, this machine learning unsupervised classification algorithm is typically used when you do not know what you are looking for and are trying to identify some clusters in your data. In its attempt at classification using K = 3 to

segment the areas of interest from the background, it has not performed well on OCT data. It has performed poorly in identifying boundaries of layers, abnormalities, and features as the clinically annotated ground truth. In a clinical setting, this automated algorithm will most likely not provide sufficient detail for an ophthalmologist thus imposing limitations on the diagnostic capability.

In the conclusion of this dissertation study a comparison will be provided against each of the chosen image segmentation algorithms/techniques, it is expected that this algorithm could be amongst one of the most poorly performing for this dataset.

7.3 Segmentation Technique 3: Simple Thresholding

7.3.1 Why the Technique Was Selected

This method of image segmentation has been called the most basic method. At times basic methods can work just as well and this is why this method was selected among the finalised set of 4 image segmentation techniques/algorithms.

7.3.2 How the Technique Works

This technique/algorithm is based on a threshold value to turn a greyscale image into a binary image. Therefore, the key to this method is to select the threshold value that are above a specific intensity level. If the pixel value is smaller than the threshold, it is set to 0, otherwise it is set to a maximum value.

OpenCV library was leveraged for this segmentation technique. First the image was converted to grayscale and then THRESH_BINARY function to apply the threshold.

7.3.3 Segmented Results & Parameters Leveraged in Technique

One of the Simple Thresholding technique/algorithm segmented images has been provided in figure 39. This image has noise reduced and some retinal layers are visible. It would require a clinical expert to advise whether this segmentation approach removes too much detail or if it is sufficient.

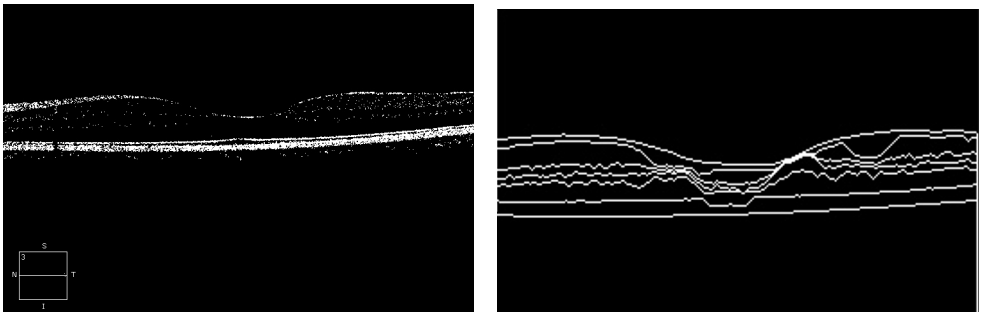

Figure 39: Simple Thresholding Segmented Image from 06 OS; Figure 27: Ground Truth Image 06 OS

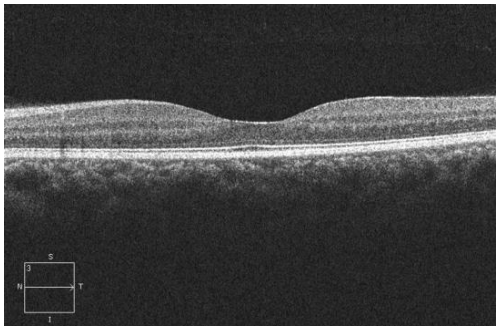

Figure 28: Original Unprocessed Image 06 OS

From direct observation of a non-clinical expert, the quality of figure 39, the Simple Thresholding segmented image, has been somewhat reduced with only 3 distinct retinal layers detected by this algorithm. There are some instances where clusters/edges are detected but a continuous persistent line is not visible from left to right across the image; these have the possibility of being partial retinal layers.

This algorithm creates visually different type of image from the ground truth (figure 27) with a reduced level of detail. Several annotated layers are missing from the segmented image. With this diminished level of detail, it would require a clinical expert to determine if this algorithm is suited for OCT data.

When comparing the segmented image to figure 28, the unprocessed image, it is clear to see a much simpler image has been created by the simple thresholding algorithm. All noise is reduced, a few retinal layers are easier to view but unfortunately other details from the image are lost.

The final parameters chosen for the threshold values in this technique/algorithm were:

- 200
- 255

These parameters offered the optimal level of detail before significant image quality was lost. It is important to note that the success seen with these parameters for the threshold values, produced varied results across all 25 unprocessed images. As all OCT images are different including their quality, although the Simple Thresholding segmented images almost completely removed speckle noise, it is the number of retinal layers the algorithm identified that varied by each segmented image. There are a small number of the 25 segmented images impacted by this.

There were other parameters that were attempted but unfortunately the segmented images were not as unsuccessful in quality. These additional attempts included parameters set at:

- THRESH_BINARY_INV function with thresholds of 200, 255
- Pre-processing attempts:
    - Applied median blur as pre-processing and threshold parameters 200, 255
    - Applied gaussian blurred as pre-processing and threshold parameters 200, 255

Figure 40: Segmented Image with Median Pre-processing; Figure 41: Segmented Image with Gaussian Pre-Processing

As seen with figures 40 and 41, the number of identified edges/clusters by the algorithm with these pre-processing techniques produced images of lower quality. The retinal layers are not as distinguishable and with figure 45 being almost non-existent. The reduced level of detail in both offer no insights into the retinal layers, features, and abnormalities.

Leveraging no pre-processing aside from converting BGR to grayscale, the final parameters of 200, 255 all 25 were applied to the simple thresholding algorithm so the segmented images could be prepared.

7.3.4 Evaluation: Dice Coefficient

For each simple thresholding segmented image, a calculation was performed for the dice coefficient to evaluate accuracy of the algorithm. The dice scores are shown below in table 3.

Segmented Image Number	Simple Threshold Dice Coefficient
1	0.335
2	0.683
3	0.37
4	0.474
5	0.478
6	0.477
7	0.414
8	0.778
9	0.481
10	0.323
11	0.528
12	0.516
13	0.488
14	0.397
15	0.512
16	0.586
17	0.345
18	0.386
19	0.347
20	0.344
21	0.354
22	0.361
23	0.75
24	0.353
25	0.547
AVG	**0.465**

Table 3: Simple Thresholding Segmentation Dice Coefficients and Average

The majority of the dice coefficient values are fairly low. There are only eight with a value higher than 0.5. This indicates that the intersection points that match between the Simple Thresholding segmented images and corresponding ground truth are slight. The values shown in table 3 align with the direct observation mentioned above, where typically 3 distinct retinal layers were detected by this algorithm and some instances where clusters/edges are detected representing partial retinal layers. However, the Simple Thresholding algorithm did produce segments that provide significant noise reduction across all 25 segmented images, and this has helped to improve the dice coefficient scores somewhat.

There are a couple of segmented images- number 8 and 23 - which are promising and perform well against the ground truth – see figures 42 to 43, 37, and 23 for results.

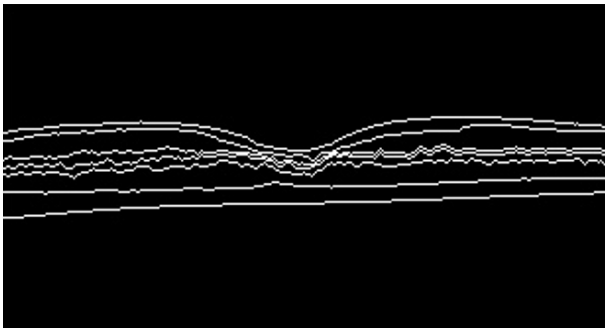

Figure 42: Ground Truth Image 198 OS; Figure 43:Segmented Image Number 8 (198 OS)

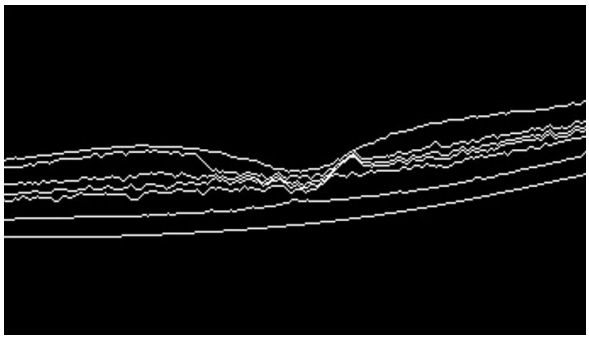

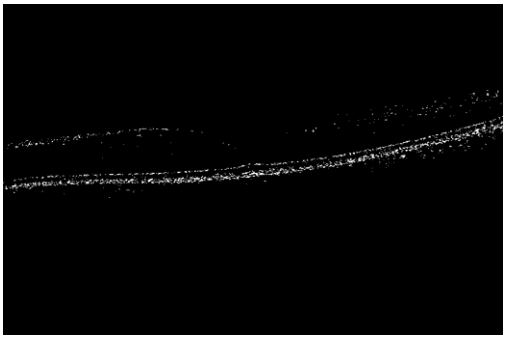

Figure 37: Ground Truth 8 macula; Figure 44: Segmented Image Number 23 (8 macula)

Although not all retinal layers across images 43 and 44 are detected, it has picked up on 3 retinal layers particularly well. Absolutely no speckle noise can be seen. For these reasons they must have overlapped well with the ground truths and produced dice coefficient values of 0.778 and 0.75. But they are far from pixel agreement perfect scores due to the layers that were not detected from the corresponding annotated ground truth images.

With this level of variability in the results, it is important to review the average. The average for Simple Thresholding algorithm is 0.465. Given how this algorithm works in how the pixel threshold is applied, it has identified some retinal layers, features, and abnormalities that the clinically annotated ground truths have. But there is a level of detail that has been completely lost by this algorithm which may prevent it from being entirely useful in clinical practice. As mentioned previously, this is an observation of a non-clinical expert, an ophthalmologist would need to advise on the success of using this algorithm in a clinical setting.

7.4 Segmentation Technique 4: Otsu's Thresholding

7.4.1 Why the Technique Was Selected

Continuing on with the thresholding image segmentation techniques/algorithm type, Otsu's Binarization thresholding method was also performed. This is the advanced method of the basic techniques and there is an expectation to have better segmented images as a result.

7.4.2 How the Technique Works

In contrast to simple thresholding, Otsu's method avoids having to choose a threshold value and determines it automatically. Otsu's method calculates the global threshold value using the image histogram to determine which pixels either fall in foreground or background. With this algorithm there are only 2 groups of pixels.

The Otsu algorithm used OpenCV, and a gaussian filter applied before using the THRESH_BINARY + THRESH_OTSU OpenCV functions.

7.4.3 Segmented Results & Parameters Leveraged in Technique

Figure 45 shows one of the Otsu's Thresholding technique/algorithm segmented images that were created. Noise seems to have been reduced fairly well. In addition, some of the quality of the retinal layers seems to have been diminished as they are not as easy to distinguish between the layers.

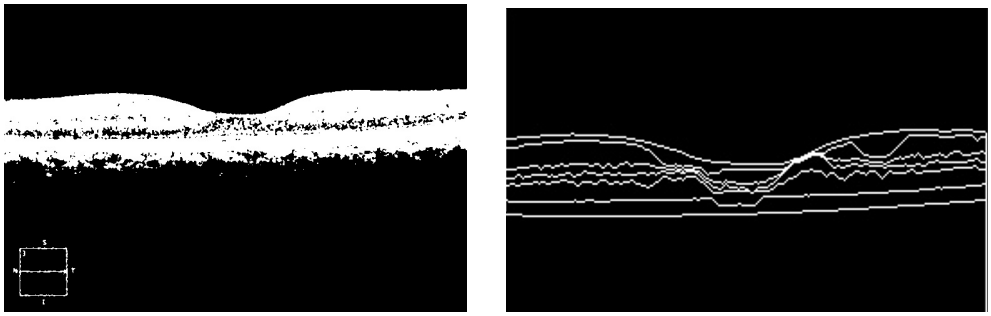

Figure 45: Otsu Thresholding Segmented Image from 06 OS; Figure 27: Ground Truth Image 06 OS

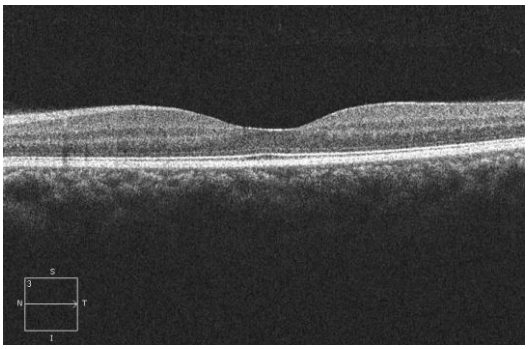

Figure 28: Original Unprocessed Image 06 OS

From direct observation of Otsu Thresholding segmented image, figure 45, it appears to have identified the retinal layers however they are all displayed in a single colour due to identifying pixels as in the foreground or background. This does create complexity in the image as the layers are not distinguishable.

When comparing figure 45 to the ground truth (figure 27), it appears all retinal layers have been detected by the algorithm which is a success, but the shape of each individual layer cannot be seen which diminishes the quality of the segmented image.

As reviewing the segmented image to figure 28, the unprocessed image, it shows Otsu Thresholding algorithm does create a much simpler image. However, there is a great level of simplification which is negatively impacting quality and possibly limiting diagnostic capability.

The final parameters chosen for this algorithm where the best results were seen are:

- Gaussian blur 5,5
- Bin 0, 255

The parameters selected provided the greatest level of detail before further image quality was compromised. Also, as seen with the other algorithms, the results produced were a variety of segments – 6 of the 25 included some level of noise, but the remaining 19 did not include noise.

Other parameters that were attempted but the segmented images were unsuccessful in quality included:

- Gaussian blur 3,3, with bin 0, 255 for thresholding
- Median filter pre-processing at kernel 3, 4, 5, with bin 0, 255 for thresholding

As can be seen in figures 46 and 47 of these attempts, speckle noise still existed in the segmented images and therefore the decision was made not to proceed with these. In particular, the median filter at a lower kernel size of 3 produced complex images with significant noise remaining within the image. The results with the median filter were slightly better but noise still was present.

Figure 46: Segmented Image with Gaussian Pre-Processing 3,3 and bin 0, 255; Figure 47: Segmented Image with Median Pre-Processing with Kernel 5

Therefore, the final parameters were leveraged to produce all 25 Otsu's thresholding segmented images ready to compare to their corresponding ground truths in the analysis step.

7.4.4 Evaluation: Dice Coefficient

Each Otsu thresholding segmented image had the dice coefficient calculated to evaluate accuracy of the algorithm. The values and the overall average for the algorithm is shown below in table 4.

Segmented Image Number	Otsu Threshold Dice Coefficient
1	0.06
2	0.055
3	0.061
4	0.061
5	0.058
6	0.069
7	0.063
8	0.078
9	0.049
10	0.061
11	0.062
12	0.051
13	0.064
14	0.062
15	0.07
16	0.056
17	0.061
18	0.06
19	0.059
20	0.06
21	0.062
22	0.061
23	0.062
24	0.062
25	0.055
AVG	**0.061**

Table 4: Otsu's Thresholding Segmentation Dice Coefficients and Average

As can be seen, the dice coefficient values are considerably low indicating limited overlapping of Otsu's Thresholding segmented images to its corresponding ground truth. The values in table 4 align with the direct observations made above, where the algorithm appears to have identified the retinal layers however they are all displayed in a single colour, creating complexity/poor quality in the image as the layers are not distinguishable. However, the algorithm does appear to have removed noise from the image.

When reviewing the dice scores, the highest value obtained is 0.078 (segmented image number 8) images, although that is still a significantly low score.

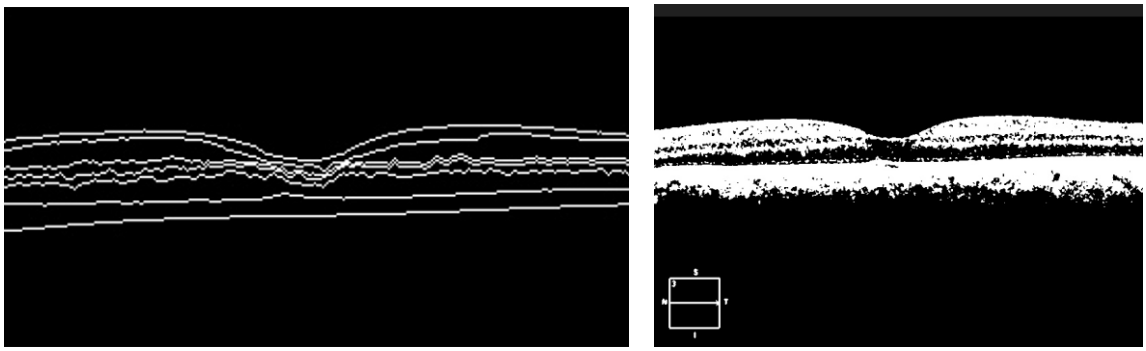

Figure 42: Ground Truth Image 198 OS; Figure 48: Segmented Image Number 8 (198 OS)

As seen in figure 48, when compared to the ground truth (figure 42), it does follow the annotated retinal layers well. Not the entire middle retinal area is in the same colour which will have helped to obtain the higher score.

In reviewing the average dice coefficient for the Otsu's Thresholding algorithm, the score of 0.061 confirms this algorithm was not suited to this dataset. Overall, it has performed poorly in identifying boundaries of layers, abnormalities, and features as the clinically annotated ground truth. It is expected that this could be amongst one of the poorly performing algorithms for this dataset.

8. Evaluation of Accuracy in Image Segmentation Techniques

Performing all 4 image segmentation techniques/algorithms across the whole dataset, has uncovered many findings, including a deeper understanding into what to expect from each techniques/algorithms according to how they are calculated and the associated segmented images they create.

In the field of ophthalmology, OCT scans need to be simplified in a particular way to be useful to clinicians. Image segmentation algorithms need to create segmented images that are as identical as possible to the annotated ground truths. The dice coefficient therefore has been leveraged in this analysis to understand the performance of the algorithm to ground truth to offer quantitative evaluation looking at the pixel-wise agreement.

Below is a recap/summary (table 5) of all coefficient values that were returned per image segmentation algorithm/technique to support the overall analysis and conclusion.

Segmented Image Number	Canny Edge Dice Coefficient	K Means Dice Coefficient	Simple Threshold Dice Coefficient	Otsu Threshold Dice Coefficient
1	0.649	0.046	0.335	0.06
2	0.281	0.064	0.683	0.055
3	0.686	0.045	0.37	0.061
4	0.65	0.043	0.474	0.061

5	0.714	0.045	0.478	0.058
6	0.731	0.045	0.477	0.069
7	0.653	0.043	0.414	0.063
8	0.841	0.055	0.778	0.078
9	0.317	0.059	0.481	0.049
10	0.657	0.045	0.323	0.061
11	0.641	0.045	0.528	0.062
12	0.287	0.06	0.516	0.051
13	0.726	0.049	0.488	0.064
14	0.668	0.045	0.397	0.062
15	0.792	0.054	0.512	0.07
16	0.308	0.065	0.586	0.056
17	0.672	0.044	0.345	0.061
18	0.661	0.045	0.386	0.06
19	0.612	0.042	0.347	0.059
20	0.671	0.043	0.344	0.06
21	0.676	0.044	0.354	0.062
22	0.679	0.043	0.361	0.061
23	0.297	0.07	0.75	0.062
24	0.634	0.044	0.353	0.062
25	0.285	0.062	0.547	0.055
AVG	**0.592**	**0.05**	**0.465**	**0.061**

Table 5: Dice Coefficients across all 4 image segmentation techniques/algorithms

A wide range of results can be seen across all 4 image segmentation methods selected for this dataset. In terms of the average dice coefficient value, Canny Edge Detection algorithm performed with the highest level of accuracy against the ground truth. The Simple Thresholding algorithm also performed well, while Ostsu Thresholding and K-Means Clustering algorithms performed the worst against the ground truth.

Canny Edge Detection algorithm does outperform the other three algorithms significantly, this therefore shows it had the greatest points of intersection across the segmented images and the corresponding annotated ground truths. This algorithm does display the greatest variability (for unknown reasons) in the range of results as the lowest value at 0.281 and highest at 0.841 for the dice coefficient. Despite this, the average is still the highest compared to the other algorithms which display less rage in the difference between highest and lowest values.

It is worth noting that Canny Edge Detection did not provide any exact matches to the ground truth. Nor is the average an exceptionally high score of something similar to 0.95+ to indicate a much greater pixel-wise agreement. Only a clinical expert will be able to advise on whether a value of 0.592 is sufficient enough to use in a clinical setting to support their analysis during diagnosis and monitoring of conditions that manifest in the retina.

The figures below provide additional reference points for insights to the average dice coefficients from table 5. Canny Edge Detection (figure 26) does offer well detected, distinct retinal layer lines as to the ground truth image and is the most simplified segmented image.

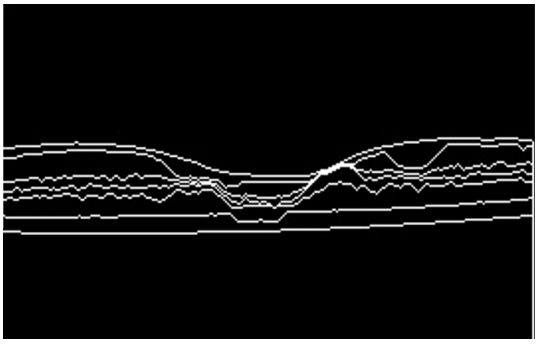

Figure 27: Ground Truth Image 06 OS

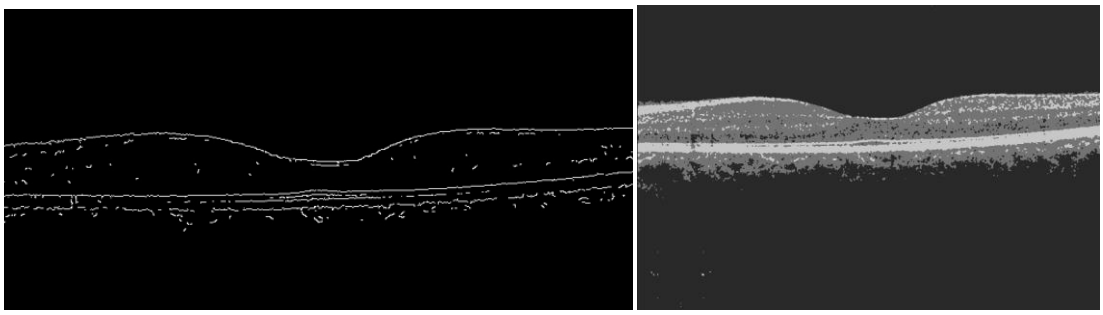

Figure 26: Canny Edge Detection Segmented Image from 06 OS; Figure 34: K-Means Clustering Segmented Image from 06 OS

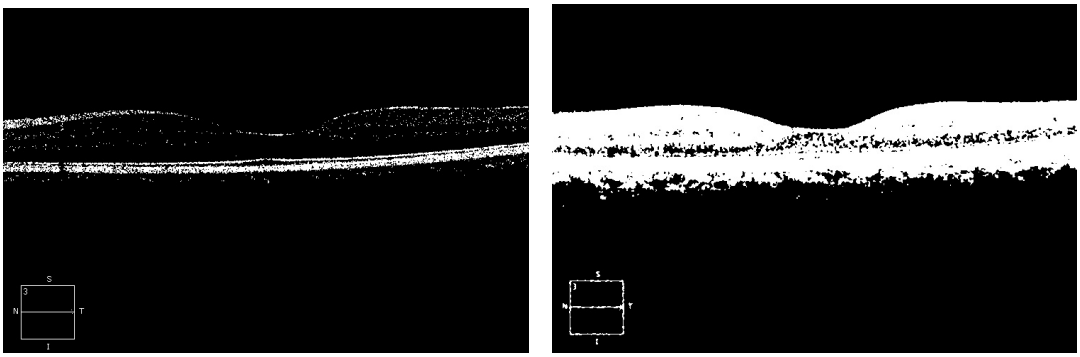

Figure 39: Simple Thresholding Segmented Image from 06 OS; Figure 45: Otsu Thresholding Segmented Image from 06 OS

Simple Thresholding, Ostsu Thresholding and K-Means Clustering algorithms do not offer as much accuracy for creating automated segments when using the average dice score, and in evaluating the figures above, it is clear to see why. They offer much more complexity in the image, too little detail, and harder to interpret. As a result, they may not be as useful for ophthalmologists to leverage these algorithms in a meaningful way for analysing OCT scans.

9. Learnings/Reflection of Data Analysis

9.1 Mat File Difficulties

While working through the data analysis, a data dictionary was not available on the data within the .mat file formats which included details on the ground truth. There were no instructions on which

data elements were of interest to leverage to compile a ground truth and being new to the subject area there was no prior experience to lean on. Attempts were made to work on the file in MatLab and Octave before moving forward in Spyder using Python.

9.2 Lack of Clinical Knowledge Challenges

Difficulties were experienced in interpreting the segmented images. Not having prior subject area expertise or access to an expert to validate learnings meant assumptions were being made that may not be entirely accurate. For example, on parameter selection for algorithms, direct observation was used – non-clinical opinion on which to proceed with using common sense but an expert could have validated if that were the best set of parameters. Also, in the evaluation when comparing segmented image to ground truth before leveraging dice score and when comparing segmented image to the unprocessed image; these were all non-expert clinical provided direct observations. Even for the most accurate algorithm, not knowing whether it is sufficient enough for an ophthalmologist expert to use.

9.3 Data Analysis General Issues

The final parameters in each algorithm worked well for some of the dataset but not all. With unstructured data, it cannot be resolved in the same way as structured data issues can. Also, the integrity of the OCT scans needed to remain intact as much as possible. As a result, some variability occurred in the segmented images.

9.4 Things That Worked Well

The algorithms selected based on knowledge developed to date, provided great variety in the range of results. The resulting segmented images made sense according to how the algorithms work. Also, leveraging the dice score as a key evaluation metric for this study allowed a quantitative perspective on how well the algorithm performed. Searching for an exact match was always going to be difficult but finding an algorithm that performs as close to an exact match of 1 as possible was the goal from the outset. The algorithm with the most overlapping intersects to the ground truth was identified.

10 Conclusion

During this quantitative analysis of image segmentation techniques/algorithms using OCT retinal images, Canny Edge Detection algorithm has proven to offer the highest accuracy of all four algorithms. It has shown the greatest potential in identifying retinal layers, features and abnormalities that are of interest to ophthalmologists that align with ground truth. Canny Edge Detection algorithm is therefore the recommended algorithm for OCT retinal images based on the dataset used for this study to support Ophthalmologists in reviewing OCT scans for diagnosis and disease monitoring.

This study has also validated that no one image segmentation method can be expected to work equally well across all images; as the results in table 5 show the Canny Edge Detection algorithm has

a range of variability across the dice coefficients of the 25 segmented images. This aligns with what was discovered during the vast research that was performed for this dissertation study.

It is important to note that despite having the highest accuracy of all four algorithms, there are additional areas of interest within the original image that are not automatically identified by the algorithm as it creates the new segmented images. This could have some limitations on the diagnostic capability using this image segmentation technique/algorithm. Given the gold standard is manual segmentation (annotated by a clinician), but it is highly time consuming, the automated Canny Edge Detection segmentation technique does still offer some benefits for ophthalmologists. A brief review of the original image may still be required by an ophthalmologist.

Searching for an exact match was always going to be difficult but finding an algorithm that performs well and has the greatest accuracy of all image segmentation techniques/algorithms that were analysed, was the goal of this dissertation study.

Also, to conclude, whilst it has been found Canny Edge Detection algorithm works well with OCT retinal scan data, the results obtained do depend on the quality of the OCT image scans in the first place. The better the quality, the better the resulting segmented images from the techniques/algorithms.

References/Appendices

1. Roger Cicala, "The Camera Versus the Human Eye", PetaPixel, NOV 17, 2012, https://petapixel.com/2012/11/17/the-camera-versus-the-human-eye/#:~:text=The%20eye%20has%20130%20million,brain%20at%20any%20given%20instant
2. Bin Qiu,Zhiyu Huang,Xi Liu, Xiangxi Meng, Yunfei You, Gangjun Liu, Kun Yang, Andreas Maier, Qiushi Ren, and Yanye Lu, "Noise reduction in optical coherence tomography images using a deep neural network with perceptually-sensitive loss function", Biomed Opt Express, 2020 Feb 1
3. Peyman Gholami, Priyanka Roy, Mohana Kuppuswamy Parthasarathy, Vasudevan Lakshminarayanan, "OCTID: Optical Coherence Tomography Image Database", arXiv preprint arXiv:1812.07056, (2018).
4. David Turbert, "What Is Optical Coherence Tomography?", American Academy of Ophthalmology, Mar. 08, 2022, https://www.aao.org/eye-health/treatments/what-is-optical-coherence-tomography
5. Dr. Louis P. Bahoshy, “What is Optical Coherence Tomography”, Stoney Creek Eye Care, https://stoneycreekeyecare.com/what-is-optical-coherence-tomography-oct/#:~:text=From%20start%20to%20finish%2C%20an,OCT%20machine%20scans%20your%20eye
6. Dr. Russel Lazarus, “What is an OCT Eye Exam”, Optometrists Network, August 23, 2020, https://www.optometrists.org/general-practice-optometry/guide-to-eye-exams/eye-exams/what-is-an-oct-eye-exam/

7. M. Matsui, T. Tashiro, K. Matsumoto, and S. Yamamoto, “A study on automatic and quantitative diagnosis of fundus photographs. I. Detection of contour line of retinal blood vessel images on color fundus photographs (author’s transl.),” Nippon Ganka Gakkai Zasshi, vol. 77, no. 8, pp. 907–918, 1973, [Online]. Available: PM:4594062.
8. G. Quellec, M. Lamard, P. M. Josselin, G. Cazuguel, B. Cochener,and C. Roux, “Optimal wavelet transform for the detection of microaneurysms in retina photographs,” IEEE Trans. Med. Imaging, vol. 27, no. 9, pp. 1230–1241, Sep. 2008.
9. Michael D. Abràmoff, Senior Member, IEEE, Mona K. Garvin, Member, IEEE, and Milan Sonka, Fellow, IEEE, "Retinal Imaging and Image Analysis", IEEE REVIEWS IN BIOMEDICAL ENGINEERING, VOL. 3, 2010
10. Michael D. Abràmoff, Senior Member, IEEE, Mona K. Garvin, Member, IEEE, and Milan Sonka, Fellow, IEEE, "Retinal Imaging and Image Analysis", IEEE REVIEWS IN BIOMEDICAL ENGINEERING, VOL. 3, 2010
11. Abrámoff, Kwon, Sonka team, "Ophthalmic Image Analysis", The Iowa Institute for Biomedical Imaging, https://www.iibi.uiowa.edu/ophthalmic-analysis
12. Su Luo, Jing Yang, Qian Gao, Sheng Zhou, Chang’an A. Zhan, "The Edge Detectors Suitable for Retinal OCT Image Segmentation", Journal of Healthcare Engineering, vol. 2017, Article ID 3978410, 13 pages, 2017. https://doi.org/10.1155/2017/3978410
13. Michael D. Abràmoff, Senior Member, IEEE, Mona K. Garvin, Member, IEEE, and Milan Sonka, Fellow, IEEE, "Retinal Imaging and Image Analysis", IEEE REVIEWS IN BIOMEDICAL ENGINEERING, VOL. 3, 2010
14. Raheleh Kafieh, Hossein Rabbani, and Saeed Kermani1, "A Review of Algorithms for Segmentation of Optical Coherence Tomography from Retina", J Med Signals Sens v.3(1); Jan-Mar 2013 PMC3785070
15. Bin Qiu, Zhiyu Huang, Xi Liu, Xiangxi Meng, Yunfei You, Gangjun Liu, Kun Yang, Andreas Maier, Qiushi Ren, and Yanye Lu, "Noise reduction in optical coherence tomography images using a deep neural network with perceptually-sensitive loss function", Biomed Opt Express. 2020 Feb 1; 11(2): 817–830.
16. Sripad Krishna Devalla, Giridhar Subramanian, Tan Hung Pham, Xiaofei Wang, Shamira Perera, Tin A. Tun, Tin Aung, Leopold Schmetterer, Alexandre H. Thiéry & Michaël J. A. Girard, "A Deep Learning Approach to Denoise Optical Coherence Tomography Images of the Optic Nerve Head", Scientific Reports, Published: 08 October 2019
17. Solomon, C.J., Breckon, T.P. (2010). “Fundamentals of Digital Image Processing: A Practical Approach with Examples in Matlab”. Wiley-Blackwell. doi:10.1002/9780470689776. ISBN978-0470844731.
18. Wikipedia source: https://en.wikipedia.org/wiki/Image_segmentation#:~:text=More%20precisely%2C%20image%20segmentation%20is,same%20label%20share%20certain%20characteristics.
19. Linda G. Shapiro and George C. Stockman (2001): “Computer Vision”, pp 279–325, New Jersey, Prentice-Hall, ISBN 0-13-030796-3
20. Barghout, Lauren, and Lawrence W. Lee. "Perceptual information processing system." Paravue Inc. U.S. Patent Application 10/618,543, filed July 11, 2003. Guo, Dazhou; Pei, Yanting; Zheng, Kang; Yu, Hongkai; Lu, Yuhang; Wang, Song (2020). "Degraded Image Semantic Segmentation With Dense-Gram Networks". IEEE Transactions on Image Processing. 29: 782–795. Bibcode:2020ITIP...29..782G. doi:10.1109/TIP.2019.2936111. ISSN 1057-7149. PMID 31449020. S2CID 201753511.
21. Guo, Dazhou; Pei, Yanting; Zheng, Kang; Yu, Hongkai; Lu, Yuhang; Wang, Song (2020). "Degraded Image Semantic Segmentation With Dense-Gram Networks". IEEE Transactions

on Image Processing. 29: 782–795. Bibcode:2020ITIP...29..782G. doi:10.1109/TIP.2019.2936111. ISSN 1057-7149. PMID 31449020. S2CID 201753511.
22. Yi, Jingru; Wu, Pengxiang; Jiang, Menglin; Huang, Qiaoying; Hoeppner, Daniel J.; Metaxas, Dimitris N. (July 2019). "Attentive neural cell instance segmentation". Medical Image Analysis. 55: 228–240. doi:10.1016/j.media.2019.05.004. PMID 31103790. S2CID 159038604
23. Alexander Kirillov, Kaiming He, Ross Girshick, Carsten Rother, Piotr Dollár (2018). "Panoptic Segmentation". arXiv:1801.00868
24. Raheleh Kafieh, Hossein Rabbani, and Saeed Kermani, "A Review of Algorithms for Segmentation of Optical Coherence Tomography from Retina", J Med Signals Sens. 2013 Jan-Mar; 3(1): 45–60.
25. Baghaie A, Yu Z, D'Souza RM. "State-of-the-art in retinal optical coherence tomography image analysis." Quant Imaging Med Surg 2015;5(4):603-617. doi: 10.3978/j.issn.2223-4292.2015.07.02
26. Q. Yang, C. A. Reisman, and Z. Wang, "Automated layer segmentation of macular OCT image scanss using dual-scale gradient information," Optics Express, vol. 18, no. 20, pp. 21293–21307, 2010.
27. Su Luo, Jing Yang, Qian Gao, Sheng Zhou, Chang'an A. Zhan, "The Edge Detectors Suitable for Retinal OCT Image Segmentation", Journal of Healthcare Engineering, vol. 2017, Article ID 3978410, 13 pages, 2017. https://doi.org/10.1155/2017/3978410
28. Source: https://dontrepeatyourself.org/post/edge-and-contour-detection-with-opencv-and-python/
29. Nagesh Singh Chauhan, "Introduction to Image Segmentation with K-Means clustering", KDnuggets on August 9, 2019, https://www.kdnuggets.com/2019/08/introduction-image-segmentation-k-means-clustering.html
30. Nagesh Singh Chauhan, "Introduction to Image Segmentation with K-Means clustering", KDnuggets on August 9, 2019, https://www.kdnuggets.com/2019/08/introduction-image-segmentation-k-means-clustering.html
31. Shapiro, Linda G. & Stockman, George C. (2002). "Computer Vision". Prentice Hall. ISBN 0-13-030796-3
32. OpenCV- Adaptive Thresholding, https://www.tutorialspoint.com/opencv/opencv_adaptive_threshold.htm#:~:text=Adaptive%20thresholding%20is%20the%20method,()%20of%20the%20Imgproc%20class
33. Sunil L. Bangare, Amruta Dubal , Pallavi S. Bangare ,Dr. S. T. Patil, "Reviewing Otsu's Method For Image Thresholding",International Journal of Applied Engineering Research, ISSN 0973-4562 Volume 10, Number 9 (2015) pp. 21777-21783
34. OpenCV, source: https://docs.opencv.org/3.4/d4/d73/tutorial_py_contours_begin.html
35. Tejas Rama, "Contour Detection & Edge Detectuib with opencv", Medium, Juk 19, 2020. Source: https://medium.com/@tejas9723/contour-detection-edge-detection-with-opencv-96a74097e1f6
36. Source: https://learnopencv.com/contour-detection-using-opencv-python-c/
37. Vamsi Krishna Madasu, Prasad Yarlagadda, "An in Depth Comparison of Four Texture Segmentation Methods," 9th Biennial Conference of the Australian Pattern Recognition Society on Digital Image Computing Techniques and Applications (DICTA 2007), 2007, pp. 366-372, doi: 10.1109/DICTA.2007.4426820.
38. Laleh Armi, Shervan Fekri-Ershad, "Texture image analysis and texture classification methods - A review", International Online Journal of Image Processing and Pattern Recognition, Vol. 2, No.1, pp. 1-29, 2019

39. Aegis, “Watershed Algorithm and its application for image segmentation”, https://www.aegissofttech.com/articles/watershed-algorithm-and-limitations.html
40. Source: https://en.wikipedia.org/wiki/Image_segmentation#Watershed_transformation
41. Aegis, “Watershed Algorithm and its application for image segmentation”, https://www.aegissofttech.com/articles/watershed-algorithm-and-limitations.html
42. Caubalejo, “Image Processing - Blob Detection”, https://towardsdatascience.com/image-processing-blob-detection-204dc6428dd
43. Caubalejo, “Image Processing - Blob Detection”, https://towardsdatascience.com/image-processing-blob-detection-204dc6428dd
44. Bashir Isa Dodo, Yongmin Li, Khalid Eltayef & Xiaohui Liu, "Automatic Annotation of Retinal Layers in Optical Coherence Tomography Images", Journal of Medical Systems, Published: 13 November 2019
45. Peyman Gholami, Priyanka Roy, Mohana Kuppuswamy Parthasarathy, Vasudevan Lakshminarayanan, "OCTID: Optical Coherence Tomography Image Database", arXiv preprint arXiv:1812.07056, (2018).
46. For more information and details about the database see: https://arxiv.org/abs/1812.07056
47. Peyman Gholami, Priyanka Roy, Mohana Kuppuswamy Parthasarathy, Vasudevan Lakshminarayanan, "OCTID: Optical Coherence Tomography Image Database", arXiv preprint arXiv:1812.07056, (2018).
48. Sourodip Kundu, "KMeans For Beginner", Median on Nov 4, 2019. Source: https://medium.com/@KunduSourodip/kmeans-for-beginner-4af96166379e
49. Nagesh Singh Chauhan, "Introduction to Image Segmentation with K-Means clustering", KDnuggets on August 9, 2019, https://www.kdnuggets.com/2019/08/introduction-image-segmentation-k-means-clustering.html